NATIONAL ADVISORY COMMITTEE FOR AERONAUTICS

TECHNICAL NOTE 3390

SECOND-ORDER SUBSONIC AIRFOIL-SECTION THEORY AND ITS PRACTICAL APPLICATION

By Milton D. Van Dyke

Ames Aeronautical Laboratory
Moffett Field, Calif.

Washington
March 1955

NATIONAL ADVISORY COMMITTEE FOR AERONAUTICS

TECHNICAL NOTE 3390

SECOND-ORDER SUBSONIC AIRFOIL-SECTION THEORY AND ITS PRACTICAL APPLICATION

By Milton D. Van Dyke

SUMMARY

Several recent advances in plane subsonic flow theory are combined into a unified second-order theory for airfoils of arbitrary shape. The solution is reached in three steps: The incompressible result is found by integration, it is converted into the corresponding subsonic compressible result by means of the second-order compressibility rule, and it is rendered uniformly valid near stagnation points by further simple rules. Solutions for a number of airfoils are given and are compared with the results of other theories and of experiment. A straightforward computing scheme is outlined for calculating the pressures on any airfoil at any angle of attack.

INTRODUCTION

Thin-airfoil theory provides a useful first approximation to the incompressible flow past two-dimensional airfoils, and the results can be immediately extended to subsonic compressible flow by the Prandtl-Glauert rule. It is natural to attempt to improve this simple theory by successive approximations so as to increase its accuracy for thicker airfoils and higher subsonic Mach numbers. There results a series expansion of the flow quantities in powers (supplemented in some cases by logarithms) of the airfoil thickness ratio, camber ratio, and angle of attack.

For incompressible flow, the higher-order theory has been studied by various writers, in particular Riegels and Wittich (refs. 1 and 2) and Keune (ref. 3). A less straightforward series of approximations was developed by Goldstein (ref. 4). Perhaps the most concise exposition of higher-order incompressible thin-airfoil theory is given by Lighthill (ref. 5).

For subsonic compressible flow, the corresponding analysis was first undertaken by Görtler (ref. 6), followed by Hantzsche and Wendt (refs. 7 and 8), Schmieden and Kawalki (ref. 9), Kaplan (refs. 10 and 11), and Imai and Oyama (refs. 12 and 13).[1] These investigators treated only specific simple shapes by rather laborious analysis. Later, it was discovered

[1]These historical references are intended to be representative rather than exhaustive.

that particular integrals of the second-order iteration equation can be expressed in terms of the first approximation (refs. 14 and 15). This permits the second-order subsonic solution for any profile to be given in terms of integrals (refs. 15 and 16). However, the resulting solutions are incorrect everywhere for airfoils with stagnation points, for reasons to be discussed later.

Recently Hayes (ref. 17), improving on a result of Imai (ref. 18), has given a second-order similarity rule for surface pressure that implies a second-order extension of the Prandtl-Glauert rule (ref. 19). This remarkable result was overlooked by earlier investigators because they did not calculate surface pressures, but were content with finding surface speeds, for which the second-order compressibility rule is more complicated. These rules reduce the second-order problem of subsonic compressible flow past airfoils to the corresponding incompressible problem.

However, the solution by successive approximations breaks down near leading and trailing edges if there are stagnation points. The result is therefore merely a formal series expansion, which fails to converge near the edges. In first-order theory spurious singularities arise at stagnation edges, but it is known how they can be taken into account, since they are integrable. In the second approximation, however, these singularities are intensified, so that at round edges they are no longer integrable. In any case, the calculated speeds and pressures are incorrect near such edges, and more so in the second approximation than the first. Moreover, in subsonic compressible flow the second approximation may be incorrect everywhere as a consequence of the defects in the first approximation.

For round edges in incompressible flow, previous investigators have shown how these defects can be corrected. Riegels (ref. 2) gave a simple rule that renders the first-order thin-airfoil solution valid near the edge. Lighthill (ref. 5) gave an equivalent rule for the second approximation. Recently, corresponding rules have been developed for higher approximations, for sharp as well as round edges, and for subsonic compressible flow (ref. 20).

It is the aim of this paper to combine these recent advances into a unified theory. There results a uniform second approximation to subsonic flow past any profile at angle of attack, expressed in terms of integrals that can, if necessary, be evaluated numerically. It may be noted that the resulting solution is now generally believed to be valid only below the critical Mach number - that is, for purely subsonic flows. Although only flow quantities at the airfoil surface are considered here in detail, the entire flow field can be treated in the same way.

For numerical computation, the method initiated by Germain (ref. 21), and extended by Watson (ref. 22), Thwaites (ref. 23), and Weber (ref. 24) appears to be the most useful. It requires a knowledge only of the airfoil ordinates at a specified set of points. A straightforward scheme, based on this method, is given for computing the second-order subsonic

solution for any airfoil. The reader interested only in calculating a specific case, without necessarily understanding the theory, can turn directly to the section "PRACTICAL NUMERICAL COMPUTATION" on page 19.

THEORY

From the preceding remarks it is clear that the solution is reached in three steps. First, the formal second-order incompressible solution is found by integration. Second, this is converted into the corresponding subsonic compressible solution by means of the second-order compressibility rule. Third, this is modified near stagnation points by the appropriate rules for round or sharp edges. These three steps will be considered successively.

Formal Incompressible Solution

The expansion of the velocity components in a formal series of powers of the airfoil thickness ratio, camber ratio, and angle of attack has been discussed in detail by Lighthill (ref. 5). It will suffice here to summarize his results for the second approximation. We mainly follow his notation except to make it more mnemonic, and to suppress his parameter ϵ characteristic of the airfoil thickness, which is only convenient in the detailed analysis.

Accordingly, consider an airfoil of moderate thickness and camber at a moderate angle of attack to a uniform subsonic stream (sketch (a)). It is essential that the x axis be chosen to pass through both the leading and trailing edges. Let the upper and lower surfaces of the airfoil be described by

$$y = Y(x) = C(x) \pm T(x) \quad (1)$$

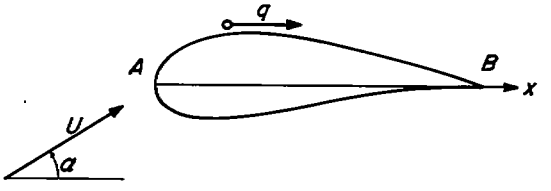

Sketch (a)

where $C(x)$ describes the mean camber line and $T(x)$ the thickness. The airfoil extends over the interval $A \leq x \leq B$, which is usually conveniently taken to be either $-1 \leq x \leq 1$ or $0 \leq x \leq 1$. All symbols are defined in Appendix A.

First-order solution.- In the first approximation of thin-airfoil theory, the condition of tangent flow at the airfoil surface is imposed on the two sides of the chord line $y = 0$ rather than at the surface, and requires that

$$\left.\frac{v_1}{U}\right|_{y=0} = Y'(x) = C'(x) \pm T'(x) \quad (2)$$

The corresponding horizontal velocity disturbance on the chord line, which is required for calculating the surface pressure, consists of a term associated with the airfoil thickness, and another associated with its camber and angle of attack. For the thickness

$$\frac{u_{1t}}{U} = \frac{1}{\pi} \oint_A^B \frac{T'(\xi)\, d\xi}{x - \xi} \tag{3}$$

and for the camber and angle of attack

$$\frac{u_{1c}}{U} = \left(\frac{B - x}{x - A}\right)^{1/2} \left[\alpha + \frac{1}{\pi} \oint_A^B \left(\frac{\xi - A}{B - \xi}\right)^{1/2} \frac{C'(\xi)\, d\xi}{x - \xi}\right] \tag{4}$$

The latter result is due to Munk (ref. 25) and the former was apparently first given by Squire in a paper that is still not generally available. Cauchy principal values are indicated in each integral.

The surface speed is then given to a first approximation by

$$\frac{q_1}{U} = 1 + \frac{u_{1t}}{U} \pm \frac{u_{1c}}{U} \tag{5}$$

Second-order solution.- In the second approximation, the tangency condition is transferred from the airfoil surface to the chord line by Taylor series expansion. The condition on the second-order increment in vertical velocity is thus found to be

$$\left.\frac{v_2}{U}\right|_{y=0} = C'_2(x) \pm T'_2(x) \tag{6a}$$

where

$$\left.\begin{aligned} C_2(x) &= \frac{u_{1t}}{U} C + \frac{u_{1c}}{U} T \\ T_2(x) &= \frac{u_{1t}}{U} T + \frac{u_{1c}}{U} C \end{aligned}\right\} \tag{6b}$$

(We depart here from Lighthill's notation in order to emphasize that the functions C_2 and T_2 are effectively the camber and thickness for some fictitious airfoil.) The problem is identical with that in first-order theory except for the condition at infinity, which is readily disposed of. Thus, corresponding to T_2 is the increment in horizontal velocity

$$\frac{u_{2t}}{U} = \frac{1}{\pi} \oint_A^B \frac{T'_2(\xi)\, d\xi}{x - \xi} - \frac{1}{2}\alpha^2 \tag{7}$$

and corresponding to C_2

$$\frac{u_{2c}}{U} = \frac{1}{\pi}\left(\frac{B - x}{x - A}\right)^{1/2} \int_A^B \left(\frac{\xi - A}{B - \xi}\right)^{1/2} \frac{C'_2(\xi)\, d\xi}{x - \xi} \tag{8}$$

The velocity components on the surface of the airfoil include also terms arising from the transfer from the chord line to the surface, which is again effected by Taylor series expansion. Hence the surface speed is given to a second approximation by

$$\frac{q_2}{U} = 1 + \frac{u_{1t}}{U} \pm \frac{u_{1c}}{U} + \frac{u_{2t}}{U} \pm \frac{u_{2c}}{U} + (C \pm T)(C'' \pm T'') + \frac{1}{2}(C' \pm T')^2 \tag{9}$$

Airfoil integrals.- The incompressible solution to second order (or, indeed, to any order) is thus reduced to a succession of "airfoil integrals" typified by equations (3), (4), (7), and (8). Goldstein (ref. 26) emphasizes that in first-order theory these integrals can be evaluated analytically for practically every profile for which formulas have ever been proposed. In second-order theory this appears to be true to a somewhat lesser extent, although the labor of calculation becomes great except for simple shapes. Often the integrals are most readily evaluated by guessing $(u - iv)$ as a function of the complex variable $(x + iy)$ that has the required behavior on the chord line. A short table of airfoil integrals useful for finding second-order solutions is given in Appendix B. Others can be found in references 26 and 27.

For complicated profiles, exact analytic evaluation of the integrals may be impossible or excessively laborious. Then numerical integration may be resorted to, or the profile can be approximated by a simpler shape that can be treated analytically. The most useful numerical procedure is apparently that originated by Germain and simplified and extended by Watson, Thwaites, and Weber. In this method the airfoil ordinates are approximated by the trigonometric polynomial

$$Y \approx c_0 + \sum_{r=1}^{N-1} (c_r \cos r\theta + t_r \sin r\theta) + c_N \cos N\theta \tag{10}$$

where θ is the angle indicated in sketch (b). The coefficients c_r (for camber) and t_r (for thickness) are chosen to give the actual ordinates at the $2N$ points for which $\theta = m\pi/N$. In this way it is found that the airfoil integrals can be expressed approximately as sums of

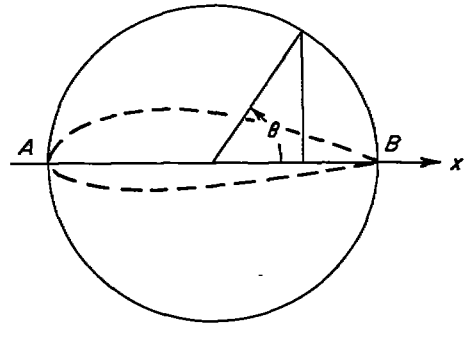

Sketch (b)

the airfoil ordinates at certain pivotal points multiplied by standard influence coefficients. The details of this method, as adapted to thin-airfoil theory, are given in Appendix C. The numerical computing procedure is outlined in the last section of this paper.

Second-Order Compressibility Rule

The second-order counterpart of the Prandtl-Glauert compressibility rule is implicit in an extension of transonic similitude that was initiated by Imai (ref. 18) and carried to completion by Hayes (ref. 17). Imai sought to improve the transonic similarity rule by retaining in its derivation all terms proportional to the square of the airfoil thickness except one appearing in the condition of tangent flow at the surface. The correlation of experimental data was not appreciably improved, which led him to suggest that the neglected second-power term should also be included. This probably cannot be done. However, in attempting merely to reproduce Imai's result as announced before publication, Hayes actually included that term in a second-order rule for surface pressure.

Hayes' result is that for two-dimensional subsonic or supersonic flow the ratio of the second-order to first-order pressure term on the surface is proportional to the parameter

$$\frac{\tau}{(|1 - M^2|)^{3/2}} \left[\frac{\gamma + 1}{2} M^4 + 2(1 - M^2) \right] \tag{11}$$

where τ is some measure of the thickness, camber, or angle of attack. Now at subsonic speeds the first-order pressure term is related to its value in incompressible flow by the Prandtl-Glauert rule. Combining these two results yields the second-order compressibility rule (ref. 19).

In incompressible flow the second-order surface-pressure coefficient has the form

$$C_{p_0}(x) = C_{p_1}(x) + \Delta C_{p_2}(x) \tag{12a}$$

where the first-order term C_{p_1} contains linear terms in thickness, camber, and angle of attack, and the second-order increment ΔC_{p_2} contains their squares and products. Then for the same airfoil in subsonic compressible flow, according to the compressibility rule, the pressure coefficient is

$$C_{p_M} = K_1 C_{p_1} + K_2(\Delta C_{p_2}) \tag{12b}$$

where

$$\left.\begin{aligned} K_1 &= \frac{1}{\sqrt{1 - M^2}} = \frac{1}{\beta} \\ K_2 &= \frac{(\gamma + 1)M^4 + 4\beta^2}{4\beta^4} \end{aligned}\right\} \tag{12c}$$

It has been pointed out that the formal thin-airfoil series requires modification near stagnation edges. The modification must in general be performed on the speed rather than the pressure. Hence the compressibility rule for surface speed is required. It is readily found from the above rule for pressure by considering the small-disturbance series form of Bernoulli's equation for compressible flow. Thus it is found that if the surface speed ratio in incompressible flow is

$$\frac{q_0}{U} = 1 + \frac{\Delta q_1}{U} + \frac{\Delta q_2}{U} \tag{13a}$$

then at subsonic speeds

$$\frac{q_M}{U} = 1 + K_1 \frac{\Delta q_1}{U} + K_2 \frac{\Delta q_2}{U} + \frac{K_2 - 1}{2} \left(\frac{\Delta q_1}{U}\right)^2 \tag{13b}$$

with

$$\frac{K_2 - 1}{2} = M^2 \frac{(\gamma + 1)M^2 + 4\beta^2}{8\beta^4} \tag{13c}$$

This rule is seen to lack the fundamental simplicity of the rule for pressure.

Modification for Stagnation Edges

Thin-airfoil theory is known to fail near leading and trailing edges if there is a stagnation point. The flow is actually brought to rest, but thin-airfoil theory predicts infinite speeds instead. If r is the distance from the edge, the velocity contains powers of $r^{-1/2}$ for a round edge and for any leading edge with flow around it (associated with angle of attack), and powers of $\ln r$ for a sharp edge. First-order theory contains first powers of these singularities, second-order theory their squares, and so on, so that the formal thin-airfoil series diverges in some neighborhood of the edge. Not only are the velocities and pressure incorrect near stagnation edges, but nonintegrable singularities appear in the higher-order expressions for aerodynamic forces.

False subsonic solutions.- Even more serious difficulties may arise in subsonic compressible flow, where the infection spreads in some cases so that the formal second-order solution is incorrect not only near the edges but over the entire airfoil surface. Thus, using the particular integral of reference 14, Harder and Klunker gave an expression for the second-order solution for any symmetric airfoil at zero angle of attack (ref. 16). However, they noted that their expression does not apply to round-edged airfoils, for which it contains divergent integrals. A more deceptive defect appears if their expression is applied to a sharp-edged airfoil such as a biconvex section; then the predicted surface speeds are finite (except near the edges) but incorrect everywhere by a term proportional to M^2. This defect arises from the fact that near the edges the first-order source distribution is not approximately the airfoil slope, as is assumed in thin-airfoil theory. The second-order solution involves the derivative of the source strength which, as indicated in sketch (c), has sharp peaks that are missed by thin-airfoil theory. It is enough to take account of this shortcoming in even the crudest fashion. Thus, if the region of integration is extended an infinitesimal distance beyond the edges to include the pulses (Dirac delta functions) of the thin-airfoil approximation, Harder and Klunker's expression yields a solution that is correct to second order except in the vicinity of the edges.

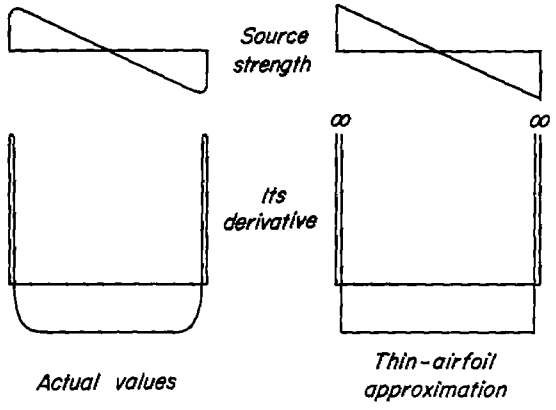

Sketch (c)

Keune has discovered an alternative particular integral containing the stream function rather than the velocity potential, and so has obtained another expression for the second-order solution (ref. 15). Because the tangency condition is one degree smoother for the stream function than the velocity potential, his expression yields the correct result (except near stagnation edges) for sharp-edged shapes. It fails, however, for round-edged shapes, so that his solution for subsonic flow past an ellipse is incorrect everywhere.

Both these expressions can be manipulated by partial integration so as to be correct except near stagnation edges. However, the result is simply that obtained by applying the second-order compressibility rule to the expressions for second-order incompressible flow. Hence these more serious difficulties are of no further concern here. They do serve, however, to warn of the danger of false second-order solutions in more complicated problems.

Modification for incompressible flow.- For round edges in incompressible flow, Riegels (ref. 2) and Lighthill (ref. 5) have given simple rules that render the formal thin-airfoil solution uniformly valid. The result

is at least a first approximation to the flow disturbances near the edge. Riegels found a rule for first-order theory by considering the conformal mapping, and Lighthill found a rule for second-order theory by considering a contraction of abscissas that shifts the thin-airfoil solution by half the radius of the edge.

In reference 20 corresponding rules have been developed for higher approximations, sharp edges, and subsonic compressible flows. The technique used there is to consider the exact solution for some simple shape that approximates the airfoil in the vicinity of its edge. The ratio of the exact solution for the simple shape to its formal thin-airfoil series expansion serves as a multiplicative factor that corrects the series expansion for the actual airfoil. The result should then be simplified insofar as possible. The relevant rules will be summarized here; the details are given in reference 20.

A round-nosed airfoil can be closely approximated by a parabola whose axis coincides with the initial camber line (sketch (d)). The exact solution for incompressible flow past the parabola (resolved into streaming and circulatory components) leads to the following rule that converts the formal second-order solution "q_2" for surface speed into a uniformly valid approximation $\bar{q}_2$:

$$\frac{\bar{q}_2}{U} = \left(\frac{x_o \pm \lambda\sqrt{2\rho x_o}}{x_o + \rho/2 \pm \lambda\sqrt{2\rho x_o}}\right)^{1/2}\left(\frac{"q_2"}{U} + \frac{\rho}{4x_o}\right) \tag{14}$$

Here x_o is the abscissa measured from the edge into the airfoil, ρ is the edge radius, λ is the initial angle of camber, and the $\pm$ signs refer, as usual, to the upper and lower surfaces.

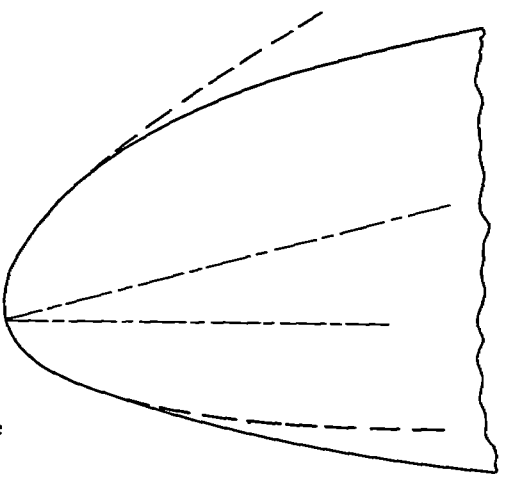

Sketch (d)

This rule yields a uniform second approximation to the disturbances everywhere (except at the other edge, where additional modification may be required) if the rate of change of curvature of the profile is continuous, which means that near the edge the thickness has the form

$$T(x) = b_1\sqrt{x_o} + b_3 x_o^{3/2} + \ldots \tag{15}$$

However, airfoils of the NACA four- and five-digit series violate this requirement, their leading edges having the initial form

$$T(x) = b_1\sqrt{x_o} + b_2 x_o + b_3 x_o^{3/2} + \ldots \tag{16}$$

Hence the rule yields only a first approximation near the edge (while leaving a second approximation elsewhere) and can therefore be replaced by the simpler form

$$\frac{\bar{q}_2}{U} = \left(\frac{x_o}{x_o + \rho/2}\right)^{1/2} \left(\frac{"q_2"}{U} + \frac{\rho}{4x_o}\right) \tag{17}$$

which is Lighthill's rule.

The rule for first-order theory is obtained by dropping the term $\rho/4x_o$ from equation (17). However, it is then advantageous to use the alternative form due to Riegels (ref. 2), which is correct to the same order but a great deal more accurate (see ref. 20). It is simply

$$\frac{\bar{q}_1}{U} = (\cos \eta) \frac{"q_1"}{U} \tag{18}$$

where η is the angle of the airfoil surface. Analogous alternative rules can be found for the second-order theory, but their shortcomings probably outweigh their slight advantages of accuracy and simplicity, so they will not be considered here.

The modification for a sharp edge is found by considering incompressible flow in an angle. If the edge is a trailing edge with Kutta condition enforced, or a leading edge at the ideal angle of attack, so that there is no flow around it, the second-order rule is

$$\frac{\bar{q}_2}{U} = x_o^{\frac{\delta}{\pi-\delta}} \left[\frac{"q_2"}{U} - \frac{\delta}{\pi} \frac{"q_1"}{U} \ln x_o - \frac{\delta^2}{\pi^2}\left(\ln x_o - \frac{1}{2} \ln^2 x_o\right)\right] \tag{19}$$

where δ is the semivertex angle, and $"q_1"$ is the first-order solution. Otherwise, the circulatory part of the formal second-order solution, which consists of the terms singular like $x_o^{-1/2}$, must first be corrected separately by the rule

$$\frac{\bar{q}_2}{U} = x_o^{\frac{\delta}{2(\pi-\delta)}} \left(\frac{"q_2"}{U} - \frac{\delta}{2\pi} \frac{"q_1"}{U} \ln x_o\right) \tag{20}$$

after which the remainder is corrected by equation (19).

Airfoils with two stagnation edges can be treated either by applying the appropriate correction separately at each edge, or by combining the rules. The combined rule for two round edges is given in equation (24) of reference 20. Similarly, for a round edge at $x = -1$ and a sharp edge (with Kutta condition) at $x = 1$, the combined rule is

$$\frac{\bar{q}_2}{U} = (1 - x)^{\frac{\delta}{\pi - \delta}} \left[\frac{1 + x \pm \lambda \sqrt{2\rho(1 + x)}}{1 + x + \rho/2 \pm \lambda \sqrt{2\rho(1 + x)}} \right]^{1/2} \left\{ \frac{"q_2"}{U} - \frac{\delta}{\pi} \frac{"q_1"}{U} \ln (1 - x) + \right.$$

$$\left. \frac{\rho}{4(1 + x)} + \frac{\delta^2}{\pi^2} \left[\frac{1}{2} \ln^2(1 - x) - \ln (1 - x) \right] \right\} \qquad (21)$$

For two sharp edges of equal angle, both with Kutta condition (as for a biconvex airfoil at zero angle of attack), and located at $x = \pm 1$, the combined rule has the form of equation (19) with x_o replaced by $(1 - x^2)$.

If the pressure is required, it must be calculated from the speed using the full Bernoulli equation because the disturbances are no longer assumed to be small.

Modification for subsonic flow.- For round noses, these rules are extended to subsonic speeds by considering compressible flow past a parabola. Thus the counterpart of equation (14) is found to be[2]

$$\frac{\bar{q}_2}{U} = Q\left(\frac{x_o \pm \lambda \sqrt{2\rho x_o}}{\rho}, \frac{a}{\sqrt{\rho/2}}, M \right) \left[\frac{"q_2"}{U} - K_1 \frac{a}{\sqrt{x_o}} \frac{"q_1"}{U} + \right.$$

$$\left. \frac{1}{4} K_2 \frac{\rho}{x_o} + \left(K_1^2 - \frac{K_2 - 1}{2} \right) \frac{a^2}{x_o} \right] \qquad (22)$$

Here, as indicated in sketch (e), Q is the speed ratio on the surface of a parabola in a uniform subsonic stream of Mach number M, with circulatory flow proportional to a. The combination $\tilde{x}_o = x_o \pm \lambda \sqrt{2\rho x_o}$ appears in the first argument of Q, as it does in equation (14), because of the connection indicated in sketch (e) between abscissas of a surface point measured along the x axis and along the axis of the parabola. (See also eq. (9) of ref. 20.) The factor a is proportional to the

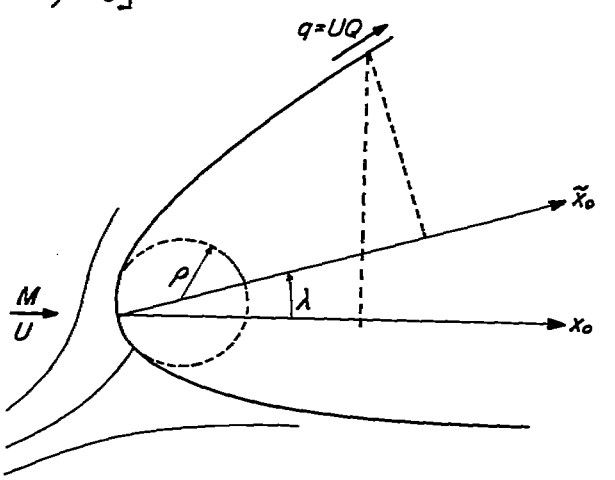

Sketch (e)

[2]It should be noted that as $M \to 0$ this rule reduces not to the incompressible rule of equation (14), but to an alternative that is entirely equivalent up to terms of second order. See footnote 7 of reference 20.

angle of attack of the actual airfoil measured from the ideal angle at which the stagnation point coincides with the vertex. It must be found as the coefficient of $x_o^{-1/2}$ in the first-order solution $"q_i"/U$.

The function Q is not known exactly, but a satisfactory approximation is given by the Janzen-Rayleigh solution in powers of M^2. For the special case of $Q\left(\frac{\tilde{x}_o}{\rho}, 0, M\right)$, corresponding to the ideal angle of attack where $a = 0$, the solution has been calculated to order M^4 by Imai (ref. 28). It is tabulated briefly in reference 20 for $\gamma = 7/5$, where it is denoted by $Q(x/\rho, M)$. For other angles of attack, the function Q to order M^2 can be extracted by a limiting process from Kaplan's solution for an inclined ellipse (ref. 29), which gives, with $\tilde{x}_o/\rho = \varphi$, $a/\sqrt{\rho/2} = \psi$

$$Q(\varphi,\psi,M) = \frac{1}{\sqrt{1 + 2\varphi}}\left[\sqrt{2\varphi} + \psi - \frac{M^2}{2(1 + 2\varphi)}\left\{(1 - \psi^2)\sqrt{2\varphi} - \psi(2\varphi + \psi^2) + \right.\right.$$

$$\frac{1 + \psi^2}{1 + 4\varphi^2}\left[\left(\sqrt{2\varphi} - \frac{1}{2}\psi + \varphi\psi\right)\ln\frac{1 + 2\varphi}{4} - \left(2\varphi - 1 - \right.\right.$$

$$\left.\left.\left.\left.2\psi\sqrt{2\varphi}\right)\tan^{-1}\sqrt{2\varphi}\right]\right\}\right] \qquad (23)$$

The rule for sharp noses in subsonic flow can be found by considering compressible flow in an angle. However, this basic solution is not yet available. For practical purposes the correction is probably negligible since it is appreciable over a much smaller neighborhood of a sharp edge than a round one. Moreover, sharp edges are usually trailing edges, in which case the details of the flow are altered by viscous effects.

EXAMPLES: COMPARISON WITH EXPERIMENT AND OTHER THEORIES

Incompressible Flow

It has been seen that the solution for subsonic flow depends on that for incompressible flow. It is therefore pertinent to test the second-order theory in the case of incompressible flow, where it can be checked against the exact results of conformal mapping.

Ellipse.- Consider an ellipse of thickness ratio τ with the interval $-1 \leq x \leq 1$ as chord line. It is described by

$$y = \pm \tau \sqrt{1 - x^2}, \qquad -1 \leq x \leq 1 \tag{24}$$

Suppose that the Kutta condition is satisfied - the rear stagnation point coincides with the end of the major axis. Then the first-order solution for surface speed is found, from equations (3), (4), and (5), together with Appendix B, to be

$$\frac{"q_1"}{U} = 1 + \tau \pm \alpha \sqrt{\frac{1 - x}{1 + x}} \tag{25a}$$

Proceeding with equations (6) to (9) gives the formal second-order result

$$\frac{"q_2"}{U} = 1 + \tau \pm \alpha \sqrt{\frac{1 - x}{1 + x}} - \frac{1}{2} \tau^2 \frac{x^2}{1 - x^2} \pm \alpha\tau \sqrt{\frac{1 - x}{1 + x}} - \frac{1}{2} \alpha^2 \tag{25b}$$

This can be checked by expanding the exact result, which is

$$\frac{q}{U} = (1 + \tau) \frac{\sqrt{1 - x^2} \cos \alpha \pm (1 - x) \sin \alpha}{\sqrt{1 - x^2 + \tau^2 x^2}} \tag{26}$$

The formal second-order solution clearly breaks down near the ends of the ellipse. It is converted into a uniformly valid second approximation by applying equation (14) twice in succession, or using the combined rule of equation (24) of reference 20, which gives

$$\frac{\overline{q}_2}{U} = \sqrt{\frac{1 - x^2}{1 - x^2 + \tau^2}} \left[(1 + \tau) \left(1 \pm \alpha \sqrt{\frac{1 - x}{1 + x}} \right) + \frac{1}{2} (\tau^2 - \alpha^2) \right] \tag{25c}$$

These approximations are compared in figure 1 with the exact solution for an 18-percent-thick ellipse (which has nearly the same nose radius as an NACA 0012 airfoil) at zero angle of attack. The precipitate descent of the formal second-order solution toward negative infinity is just discernible near the nose and is eliminated in the modified theory. It should be mentioned that the first-order theory modified according to Riegels' rule (eq. (18)) happens to give the exact result for an ellipse.

Symmetrical Joukowski airfoil.- To second as well as first order a symmetrical Joukowski airfoil of thickness ratio τ is described by

$$\left.\begin{aligned} y &= \pm\, \tau_1(1 - x)\sqrt{1 - x^2}, \qquad -1 \le x \le 1 \\ \tau_1 &= \frac{4}{3\sqrt{3}}\,\tau = 0.7698\tau \end{aligned}\right\} \tag{27}$$

By the foregoing procedure, the formal second-order solution is found to be

$$\frac{"q_2"}{U} = 1 + \tau_1(1 - 2x) \pm \alpha\sqrt{\frac{1 - x}{1 + x}} - \frac{1}{2}\,\tau_1^2\,\frac{1 - x}{1 + x}\,(1 + 2x)^2 \mp$$

$$2\tau_1\alpha x\sqrt{\frac{1 - x}{1 + x}} - \frac{1}{2}\,\alpha^2 \tag{28a}$$

where the first three terms give the first-order solution. Modifying this according to equation (14) with $x_0 = 1 + x$ and $\rho = 4\tau_1^2$ (and $\lambda = 0$) gives the uniformly valid second approximation

$$\frac{\bar{q}_2}{U} = \sqrt{\frac{1 + x}{1 + x + 2\tau_1^2}}\left[1 + \tau_1(1 - 2x) + \frac{1}{2}\,\tau_1^2(1 - 2x)^2 \pm\right.$$

$$\left.\alpha(1 - 2\tau_1 x)\sqrt{\frac{1 - x}{1 + x}} - \frac{1}{2}\,\alpha^2\right] \tag{28b}$$

In figure 2 these approximations are compared with the exact solution (ref. 30) for a 12-percent-thick section at zero angle of attack. The effect of the modification on the second-order result is not discernible to this scale.

Biconvex airfoil.- To second order a symmetrical biconvex airfoil of thickness ratio τ bounded by either circular or parabolic arcs is described by

$$y = \pm\, \tau(1 - x^2), \qquad -1 \le x \le 1 \tag{29}$$

The formal second-order solution is found to be

$$\frac{"q_2"}{U} = 1 + \frac{2}{\pi}\tau\left(2 - x \ln\frac{1+x}{1-x}\right) \pm \alpha\sqrt{\frac{1-x}{1+x}} + \tau^2\left[\frac{3}{\pi^2}\left(2 - x\ln\frac{1+x}{1-x}\right)^2 - \right.$$

$$\left.\frac{1}{\pi^2}\ln^2\frac{1+x}{1-x} - (1-x^2)\right] \mp \frac{1}{\pi}\alpha\tau\sqrt{\frac{1-x}{1+x}}\left[(1+2x)\ln\frac{1+x}{1-x} - 4\right] - \frac{1}{2}\alpha^2 \tag{30a}$$

In deducing from this a uniformly valid second approximation, the terms independent of α are treated by the rule for combined equally sharp edges that was described just after equation (21), with $\delta = 2\tau$. The terms in α are modified according to equation (20) with $x_0 = 1 + x$. (Notice that no modification of these terms is required at the trailing edge.) The result is

$$\frac{\bar{q}_2}{U} = (1-x^2)^{\frac{2\tau}{\pi-2\tau}}\left\{1 + \frac{2}{\pi}\tau\left[2 - (1+x)\ln(1+x) - (1-x)\ln(1-x)\right] + \right.$$

$$\left(\frac{2}{\pi}\tau\right)^2\left[3 - \frac{\pi^2}{4}(1-x^2) - 3(1+x)\ln(1+x) - 3(1-x)\ln(1-x) + \right.$$

$$\frac{1}{4}(1+3x)(1+x)\ln^2(1+x) + \frac{1}{4}(1-3x)(1-x)\ln^2(1-x) +$$

$$\left.\left.\frac{3}{2}(1-x^2)\ln(1+x)\ln(1-x)\right] - \frac{1}{2}\alpha^2\right\} \pm \alpha\sqrt{\frac{1-x}{1+x}}(1+x)^{\frac{\tau}{\pi-2\tau}}\left\{1 - \right.$$

$$\left.\frac{\tau}{\pi}\left[2(1+x)\ln(1+x) - (1+2x)\ln(1-x) - 4\right]\right\} \tag{30b}$$

These approximations are compared in figure 3 with the exact solution (ref. 31) for a circular-arc airfoil 18 percent thick at zero angle of attack. Although the vertex angles are large in this example, the modification of the second-order solution is appreciable in such a small neighborhood of the edge that it would be invisible even on a much larger plot.

NACA OOXX airfoils.- Symmetrical airfoils of the NACA OOXX family (such as the NACA 0012) are naturally defined for the interval $0 \le x \le 1$. The airfoil of thickness ratio τ is described by (ref. 32)

$$y = \pm T(x) = \pm\tau(b_1\sqrt{x} + b_2x + b_4x^2 + b_6x^3 + b_8x^4), \qquad 0 \le x \le 1 \tag{31}$$

where

$$b_1 = 1.48450$$
$$b_2 = -0.63000$$
$$b_4 = -1.25800$$
$$b_6 = 1.42150$$
$$b_8 = -0.50750$$

With the aid of Appendix B the first-order solution is found to be

$$\frac{"q_1"}{U} = 1 + \frac{\tau}{\pi}\left[\frac{1}{\tau}T'(x)\ln\frac{x}{1-x} + \frac{b_1}{\sqrt{x}}\ln\frac{1+\sqrt{x}}{\sqrt{x}} - 2b_4 - \frac{3}{2}b_6 - \frac{4}{3}b_8 - (3b_6 + 2b_8)x - 4b_8x^2\right] \pm \alpha\sqrt{\frac{1-x}{x}} \tag{32a}$$

in agreement with the result given by Goldstein (ref. 26). Applying Riegels' rule (eq. (18)) renders this a uniformly valid first approximation except very near the trailing edge.

The second-order terms in thickness, in addition to being very complicated, involve integrals that apparently cannot be evaluated in terms of tabulated functions. Accordingly, the second-order terms have been calculated using the Germain-Watson-Thwaites-Weber numerical method discussed in Appendix C, with N = 16. The accuracy of this approximation is assured by the fact that cruder approximations modify the numerical results only slightly, as will be seen in a later example.

The formal second-order solution for surface speed therefore has the form

$$\frac{"q_2"}{U} = 1 + \tau Q_\tau \pm \alpha\sqrt{\frac{1-x}{x}} + \tau^2 Q_{\tau\tau} \pm \tau\alpha Q_{\tau\alpha} - \frac{1}{2}\alpha^2 \tag{32b}$$

where values of Q_τ from equation (32a) and approximate numerical values of $Q_{\tau\tau}$ and $Q_{\tau\alpha}$ are

x	Q_τ	$Q_{\tau\tau}$	$Q_{\tau\alpha}$	x	Q_τ	$Q_{\tau\tau}$	$Q_{\tau\alpha}$
0.025	1.943	-9.00	8.80	0.50	0.900	-0.135	0.32
.05	1.836	-3.35	5.55	.60	.697	-.220	.11
.10	1.714	-1.00	3.25	.70	.485	-.315	-.08
.20	1.510	-.090	1.65	.80	.238	-.410	-.23
.30	1.309	.010	1.00	.90	-.124	-.420	-.33
.40	1.106	-.060	.58	.95	-.440	-.360	-.34

Applying equation (14) with $\rho = 1.10187\ \tau^2$, $\delta = 1.16925\ \tau$ (and $\lambda = 0$) yields a uniformly valid approximation. However, as discussed previously, the curvature of the profile does not vary continuously near its nose, so the result is only a first approximation there, though a second approximation elsewhere.

The various approximations are compared in figure 4 with the result of a "long and elaborate calculation" by conformal mapping for the NACA 0012 airfoil that is given by Goldstein (ref. 33). Again the effect of modifying the second-order solution is indiscernible. Also shown is the "exact" solution tabulated in reference 34. The agreement between the first-order solution with Riegels' rule, the second-order solutions, and Goldstein's calculation leaves little doubt that his is the more accurate of the two "exact" solutions.

Compressible Flow

When extended to subsonic compressible flow, the preceding examples can all be compared with other theories or with experiment. As before, the comparisons will, for simplicity, be made only for zero angle of attack.

Ellipse.- Applying the second-order compressibility rule of equations (13) to the incompressible solution of equation (25b) gives as the formal second-order solution for the speed on an elliptic cylinder

$$\frac{"q_2"}{U} = 1 + K_1\left(\tau \pm \alpha\sqrt{\frac{1-x}{1+x}}\right) + \frac{1}{2}\tau^2\left(K_2\frac{1-2x^2}{1-x^2} - 1\right) \pm$$

$$\tau\alpha(2K_2 - 1)\sqrt{\frac{1-x}{1+x}} - \alpha^2\frac{1 + (2K_2 - 1)x}{2(1+x)} \qquad (33)$$

For zero angle of attack the maximum speed, occurring at midchord, is given by

$$\left(\frac{"q_2"}{U}\right)_{max} = 1 + K_1\tau + \frac{1}{2}(K_2 - 1)\tau^2 \qquad (34)$$

in agreement with the result of Hantzsche and Wendt (ref. 7). Hantzsche has also calculated the third-order solution for the maximum speed at zero angle of attack (ref. 8). Values of the maximum speed ratio calculated from these and other approximations for a 10-percent-thick ellipse at zero angle of attack are

	M = 0.70	M = 0.75	M = 0.80
First-order theory (or Prandtl-Glauert rule applied to exact incompressible value of 1.100)	1.140	1.151	1.167
Kármán-Tsien rule	1.148	1.166	1.184
Second-order theory	1.151	1.166	1.189
Third-order theory	1.151	1.172	1.198

Here the Kármán-Tsien rule has been applied to the exact incompressible value of the pressure coefficient, and the speed ratio then calculated from Bernoulli's equation. It is to be anticipated that second-order theory is more accurate than any of the compressibility correction formulas such as the Kármán-Tsien rule, because it allows for a dependence on the particular airfoil shape and on the value of γ. This is seen to be true for the ellipse.

In the same way the second-order solutions are readily calculated for the Joukowski and the biconvex airfoils, and are found to agree with the results that Hantzsche and Wendt obtained by laborious analysis.

NACA 0012 airfoil.- The formal first- and second-order solutions for NACA 00XX airfoils in subsonic flow are easily obtained from equations (13) and (32). The second-order solution can then be rendered uniformly valid near the nose using equation (22), although again the modification is significant in only a very small region of the nose.

For the NACA 0012 airfoil at zero angle of attack, Emmons has calculated the flow field at Mach numbers of 0, 0.70, and 0.75 using the numerical relaxation method (ref. 35). The last of these Mach numbers is supercritical, so that the flow contains shock waves, and is beyond the scope of the present theory. The pressure distribution calculated by the relaxation method for $M = 0.70$ is compared in figure 5 with the results of first- and second-order theory and various other approximations. The relaxation solution for incompressible flow is also shown in comparison with Goldstein's "exact" solution, and is seen to be inaccurate near the nose. The solution for $M = 0.70$ probably contains similar inaccuracies, however, just as for the ellipse the pressure coefficients calculated by second-order theory may be slightly less negative than the true values near their minimum.

Experiments on NACA 0015 airfoil.- Experimental pressure distributions in two-dimensional flow over the NACA 0015 airfoil at high subsonic speeds are reported in reference 36. For zero angle of attack, the critical Mach number is approximately 0.70. The measurements at this Mach number are compared in figure 6 with the results of first- and second-order

theory and of the two common compressibility correction formulas applied to the incompressible flow values tabulated in reference 34. Unfortunately, the model was imperfectly constructed, and the ordinates were inaccurate near the nose and midchord. Otherwise, the measured pressures are in satisfactory accord with either second-order theory or the results of the Kármán-Tsien rule.

PRACTICAL NUMERICAL COMPUTATION

The following computing procedure yields the formal second-order subsonic solution for the surface speed or pressure on any airfoil at any angle of attack. It requires a knowledge only of the airfoil ordinates at seven points along the chord. It is based on the foregoing theory together with the numerical method of Germain, Watson, Thwaites, and Weber that is discussed in Appendix C.

Computing Procedure (N = 8)

(1) Tabulate the ordinates Y_u and Y_l of the upper and lower surfaces at the seven pivotal points x_n listed in table I. (The x axis must pass through the leading and trailing edges.)

(2) Calculate the corresponding values of

$$T = \frac{1}{2}(Y_u - Y_l), \qquad C = \frac{1}{2}(Y_u + Y_l) \tag{35}$$

(3) Using the influence coefficients of tables II and III, calculate

$$\left.\begin{aligned} \frac{u_{1t}}{U} &= \sum_{s=1}^{7} c_{ns}T_s & \frac{u_{1c}^*}{U} &= \sum_{s=1}^{7} d_{ns}C_s \\ T' &= \sum_{s=1}^{7} e_{ns}T_s & C' &= \sum_{s=1}^{7} f_{ns}C_s \\ T'' &= \sum_{s=1}^{7} g_{ns}T_s & C'' &= \sum_{s=1}^{7} h_{ns}C_s \end{aligned}\right\} \tag{36}$$

4. Using table I (with α in radians), calculate

$$\frac{u_{1c}}{U} = \frac{u_{1c}^*}{U} + \alpha \sqrt{\frac{1 - x}{x}} \tag{37}$$

5. Calculate

$$T_2 = \frac{u_{1t}}{U} T + \frac{u_{1c}}{U} C, \qquad C_2 = \frac{u_{1t}}{U} C + \frac{u_{1c}}{U} T \tag{38}$$

6. Using the influence coefficients of tables II and III, calculate

$$\frac{u_{2t}}{U} = \sum_{s=1}^{7} c_{ns} T_{2s} - \frac{1}{2} \alpha^2, \qquad \frac{u_{2c}}{U} = \sum_{s=1}^{7} d_{ns} C_{2s} \tag{39}$$

7. Using the compressibility factors of table IV, calculate

$$\frac{"q"}{U} = 1 + K_1 \frac{u_{1t}}{U} + K_2\left(\frac{u_{2t}}{U} + CC" + TT" + \frac{1}{2} C'^2 + \frac{1}{2} T'^2\right) +$$

$$\frac{K_2 - 1}{2}\left[\left(\frac{u_{1t}}{U}\right)^2 + \left(\frac{u_{1c}}{U}\right)^2\right] \pm \left[K_1 \frac{u_{1c}}{U} + K_2\left(\frac{u_{2c}}{U} + CT" + \right.\right.$$

$$\left.\left. C"T + C'T'\right) + (K_2 - 1) \frac{u_{1t}}{U} \frac{u_{1c}}{U}\right] \tag{40}$$

or

$$"C_{p_2}" = -2K_1\left(\frac{u_{1t}}{U} \pm \frac{u_{1c}}{U}\right) - K_2\left[2 \frac{u_{2t}}{U} \pm 2 \frac{u_{2c}}{U} + 2(C \pm T)(C" \pm T") - \right.$$

$$\left. (C' \pm T')^2 - \left(\frac{u_{1t}}{U} \pm \frac{u_{1c}}{U}\right)^2\right] \tag{41}$$

The $\pm$ signs refer to the upper and lower surfaces of the airfoil.

Remarks

1. The summations of steps (3) and (6) are conveniently carried out by tabulating C and T in columns that can be matched with successive columns of tables II and III while cumulative multiplication is carried out on a desk calculating machine.

2. If the airfoil slope and second derivative can be found more directly, step (3) can be simplified by omitting the calculation of T', C', T", and C".

3. The results near the nose can be rendered valid by the use of the modification of equation (22), but the effect is often insignificant.

4. Seven pivotal points yield sufficient accuracy for most purposes. If conditions near the nose of a thin airfoil are of interest it may be necessary to repeat the computation using 15 pivotal points. (The values of T and C already calculated can be used again.) Table I gives the additional pivotal points and angle-of-attack solution, and table V gives the influence coefficients for calculating u/U; additional tables can be prepared for calculating the airfoil slope and curvature if they are not known otherwise.

5. The above scheme is designed for calculating a single case. If the same airfoil is to be calculated at more than two angles of attack, it is economical to subdivide the computing scheme to separate terms in α and α^2. Similarly, the scheme should be subdivided if more than two thickness or camber ratios are to be calculated for the same family of airfoils.

6. For NACA airfoils T is the basic thickness and C the camber line. To second order it is immaterial that the thickness is added normal to the camber line rather than to the chord line.

Example

The following table gives the complete computing sheet for calculating the first- and second-order increments in surface speed for an NACA 00XX airfoil (of unit thickness ratio) at zero angle of attack and zero Mach number:

n	x	T	$\frac{u_{1t}}{U} = \frac{\Delta q_1}{U}$	T'	T"	T_2	$\frac{u_{2t}}{U}$	$\frac{\Delta q_2}{U}$
1	0.03806	0.26316	1.8936	3.0914	-54.721	0.49832	4.8040	-4.8180
2	.14645	.44236	1.6158	.8652	-8.928	.71478	3.1691	-.4062
3	.30866	.49990	1.2906	-.0235	-3.636	.64517	1.8200	.0028
4	.50000	.44051	.9053	-.5445	-1.939	.39879	.5719	-.1340
5	.69134	.30843	.4909	-.8063	-1.048	.15142	-.3081	-.3063
6	.85355	.16199	.0824	-1.0163	-1.574	.01335	-.6913	-.4298
7	.96194	.04499	-.5951	-1.0879	1.643	-.02677	-.9888	-.3230

The accuracy of this solution with only seven pivotal points is indicated by comparison with the following values, which were obtained analytically for $\Delta q_1/U$ and with 15 pivotal points for $\Delta q_2/U$:

x	$\frac{u_{1t}}{U} = \frac{\Delta q_1}{U}$	$\frac{\Delta q_2}{U}$
0.14645	1.6166	-0.4009
.50000	.9003	-.1348
.85355	.0725	.4239

It is seen that the solution using seven pivotal points yields ample accuracy.

Ames Aeronautical Laboratory
National Advisory Committee for Aeronautics
Moffett Field, Calif., Dec. 1, 1954

APPENDIX A

NOTATION

A,B	abscissas of leading and trailing edges, respectively
a	factor proportional to angle of attack measured from ideal angle
b_n	coefficient of $x^{n/2}$ in series for airfoil ordinate
$C(x)$	camber of airfoil
$C_2(x)$	camber of fictitious airfoil in second-order solution
C_p	surface-pressure coefficient
C_{p_1}	first-order surface-pressure coefficient
ΔC_{p_2}	second-order increment in surface-pressure coefficient
$c_{ns},d_{ns},e_{ns},f_{ns},g_{ns},h_{ns},$	influence coefficients for calculating velocity, slope, and second derivative of airfoil ordinate
c_r	coefficient in trigonometric polynomial approximation to C
$f(z)$	analytic function of complex variable
I	imaginary part of $f(z)$ on unit circle
K_1	first-order compressibility factor, $\frac{1}{\beta}$
K_2	second-order compressibility factor, $\frac{(\gamma + 1)M^4 + 4\beta^2}{4\beta^4}$
M	free-stream Mach number
N	number of subdivisions of chord line in numerical integration
Q	surface speed ratio on parabola in subsonic flow
$Q_T,Q_{TT},Q_{T\alpha}$	(See eq. (32b).)
q	flow speed on surface of airfoil
$\Delta q_1,\Delta q_2$	first- and second-order increments in q

R	real part of $f(z)$ on unit circle
$T(x)$	thickness of airfoil
$T_2(x)$	thickness of fictitious airfoil in second-order solution
t_r	coefficient in trigonometric polynomial approximation to T
U	free-stream speed
u	velocity perturbation parallel to chord line
v	velocity perturbation normal to chord line
x	abscissa
x_o	abscissa measured from edge into airfoil
$\tilde{x}_o$	distance from round edge measured along initial tangent to camber line
$Y(x)$	ordinate of airfoil
Y_u, Y_l	ordinates of upper and lower surfaces of airfoil, respectively
y	ordinate
z	complex variable
α	angle of attack
β	$\sqrt{1 - M^2}$
β_p	coefficient in numerical calculation of u
γ	adiabatic exponent of gas
γ_p	coefficient in numerical calculation of Y'
δ	semivertex angle of sharp edge
θ	polar angle
η	angle of airfoil surface to chord line
λ	terminal angle of camber line to chord line
μ_p	coefficient in numerical calculation of Y''

ν	factor that is 1 or $\frac{1}{2}$ (See eq. (C12).)
ρ	radius of round edge
τ	airfoil thickness ratio
τ_1	$\frac{4}{3\sqrt{3}}\tau$ for Joukowski airfoil
φ	$\frac{\tilde{x}_o}{\rho}$, also (in Appendix C) perturbation velocity potential
ψ	$\frac{a}{\sqrt{\rho/2}}$, also (in Appendix C) perturbation stream function
$(\ )_o$	value at zero Mach number
$(\ )_M$	value at Mach number M
$(\ )_1$	first-order approximation
$(\ )_2$	second-order approximation
$(\ )_t$	component associated with thickness
$(\ )_c$	component associated with camber and angle of attack
"( )"	formal series approximation
$\overline{(\ )}$	uniformly valid approximation
$(\ )^*$	part not involving angle of attack
$(\ )'$	derivative
$(\ )_m$	value at mth pivotal point counted from trailing edge
$(\ )_n$	value at nth pivotal point counted from leading edge
$(\ )_p$	index of summation, counted from trailing edge
$(\ )_s$	index of summation, counted from leading edge

APPENDIX B

AIRFOIL INTEGRALS

The following are the Cauchy principal values for $x^2 \leq 1$:

1. $$\int_{-1}^{1} \frac{1}{x-\xi}\,d\xi = \ln\frac{1+x}{1-x}$$

2. $$\int_{-1}^{1} \frac{\xi}{x-\xi}\,d\xi = x\ln\frac{1+x}{1-x} - 2$$

3. $$\int_{-1}^{1} \frac{\xi^2}{x-\xi}\,d\xi = x\left(x\ln\frac{1+x}{1-x} - 2\right)$$

4. $$\int_{-1}^{1} \frac{\xi^3}{x-\xi}\,d\xi = x^2\left(x\ln\frac{1+x}{1-x} - 2\right) - \frac{2}{3}$$

5. $$\int_{-1}^{1} \frac{\xi^n}{x-\xi}\,d\xi = x\int_{-1}^{1} \frac{\xi^{n-1}}{x-\xi}\,d\xi - \frac{1-(-1)^n}{n}$$

6. $$\int_{-1}^{1} \frac{1}{\sqrt{1-\xi^2}\,(x-\xi)}\,d\xi = 0$$

7. $$\int_{-1}^{1} \frac{\xi}{\sqrt{1-\xi^2}\,(x-\xi)}\,d\xi = -\pi$$

8. $$\int_{-1}^{1} \frac{\xi^2}{\sqrt{1-\xi^2}\,(x-\xi)}\,d\xi = -\pi x$$

9. $$\int_{-1}^{1} \frac{\xi^3}{\sqrt{1-\xi^2}\,(x-\xi)}\,d\xi = -\pi\left(x^2 + \frac{1}{2}\right)$$

10. $$\int_{-1}^{1} \frac{\xi^4}{\sqrt{1-\xi^2}\,(x-\xi)}\,d\xi = -\pi x\left(x^2 + \frac{1}{2}\right)$$

11. $$\oint_{-1}^{1} \frac{\xi^5}{\sqrt{1-\xi^2}\,(x-\xi)}\,d\xi = -\pi\left(x^4 + \frac{1}{2}x^2 + \frac{3}{8}\right)$$

12. $$\oint_{-1}^{1} \frac{\xi^6}{\sqrt{1-\xi^2}\,(x-\xi)}\,d\xi = -\pi x\left(x^4 + \frac{1}{2}x^2 + \frac{3}{8}\right)$$

13. $$\oint_{-1}^{1} \frac{\xi^n}{\sqrt{1-\xi^2}\,(x-\xi)}\,d\xi = x\oint_{-1}^{1} \frac{\xi^{n-1}}{\sqrt{1-\xi^2}\,(x-\xi)}\,d\xi - \frac{\pi}{2}\left[1-(-1)^n\right]\frac{1(3)\ldots(n-2)}{2(4)\ldots(n-1)}$$

14. $$\oint_{-1}^{1} \frac{\sqrt{1-\xi^2}}{x-\xi}\,d\xi = \pi x$$

15. $$\oint_{-1}^{1} \frac{\xi\sqrt{1-\xi^2}}{x-\xi}\,d\xi = \pi\left(x^2 - \frac{1}{2}\right)$$

16. $$\oint_{-1}^{1} \frac{\xi^2\sqrt{1-\xi^2}}{x-\xi}\,d\xi = \pi x\left(x^2 - \frac{1}{2}\right)$$

17. $$\oint_{-1}^{1} \frac{\xi^3\sqrt{1-\xi^2}}{x-\xi}\,d\xi = \pi\left(x^4 - \frac{1}{2}x^2 - \frac{1}{8}\right)$$

18. $$\oint_{-1}^{1} \frac{\sqrt{1+\xi}}{\sqrt{1-\xi}\,(x-\xi)}\,d\xi = -\pi$$

19. $$\oint_{-1}^{1} \frac{\ln\frac{1+\xi}{1-\xi}}{x-\xi}\,d\xi = \frac{1}{2}\left(\ln^2\frac{1+x}{1-x} - \pi^2\right)$$

20. $$\oint_{-1}^{1} \frac{\xi\ln\frac{1+\xi}{1-\xi}}{x-\xi}\,d\xi = \frac{1}{2}x\left(\ln^2\frac{1+x}{1-x} - \pi^2\right)$$

21. $$\oint_{-1}^{1} \frac{\xi^2\ln\frac{1+\xi}{1-\xi}}{x-\xi}\,d\xi = \frac{1}{2}x^2\left(\ln^2\frac{1+x}{1-x} - \pi^2\right) - 2$$

22. $$\oint_{-1}^{1} \frac{\xi^3 \ln\frac{1+\xi}{1-\xi}}{x-\xi}\,d\xi = \frac{1}{2}x^3\left(\ln^2\frac{1+x}{1-x} - \pi^2\right) - 2x$$

23. $$\oint_{-1}^{1} \frac{\xi^4 \ln\frac{1+\xi}{1-\xi}}{x-\xi}\,d\xi = \frac{1}{2}x^4\left(\ln^2\frac{1+x}{1-x} - \pi^2\right) - 2x^2 - \frac{4}{3}$$

24. $$\oint_{-1}^{1} \frac{\xi^n \ln\frac{1+\xi}{1-\xi}}{x-\xi}\,d\xi = x\int_{-1}^{1} \frac{\xi^{n-1} \ln\frac{1+\xi}{1-\xi}}{x-\xi}\,d\xi - \frac{2}{n}\left[1-(-1)^{n-1}\right]\sum_{\nu=0}^{\frac{n}{2}-1}\frac{1}{n-1-2\nu}$$

25. $$\oint_{-1}^{1} \frac{1}{\sqrt{1+\xi}\,(x-\xi)}\,d\xi = \frac{1}{\sqrt{1+x}}\ln\frac{\sqrt{2}+\sqrt{1+x}}{\sqrt{2}-\sqrt{1+x}}$$

26. $$\oint_{-1}^{1} \frac{\sqrt{1+\xi}}{x-\xi}\,d\xi = \sqrt{1+x}\ln\frac{\sqrt{2}+\sqrt{1+x}}{\sqrt{2}-\sqrt{1+x}} - 2\sqrt{2}$$

27. $$\oint_{-1}^{1} \frac{\ln\frac{1+\xi}{1-\xi}}{\sqrt{1-\xi^2}\,(x-\xi)}\,d\xi = -\frac{\pi^2}{\sqrt{1-x^2}}$$

28. $$\oint_{-1}^{1} \frac{\xi \ln\frac{1+\xi}{1-\xi}}{\sqrt{1-\xi^2}\,(x-\xi)}\,d\xi = -\pi^2\frac{x}{\sqrt{1-x^2}}$$

29. $$\oint_{-1}^{1} \frac{\xi^2 \ln\frac{1+\xi}{1-\xi}}{\sqrt{1-\xi^2}\,(x-\xi)}\,d\xi = -\pi\left(2 + \pi\frac{x^2}{\sqrt{1-x^2}}\right)$$

30. $$\oint_{-1}^{1} \frac{\xi^3 \ln\frac{1+\xi}{1-\xi}}{\sqrt{1-x^2}\,(x-\xi)}\,d\xi = -\pi x\left(2 + \pi\frac{x^2}{\sqrt{1-x^2}}\right)$$

31. $$\oint_{-1}^{1} \frac{\xi^4 \ln\frac{1+\xi}{1-\xi}}{\sqrt{1-\xi^2}\,(x-\xi)}\,d\xi = -\pi\left(\frac{5}{3} + 2x^2 + \pi\frac{x^4}{\sqrt{1-x^2}}\right)$$

32. $$\oint_{-1}^{1} \frac{\xi^n \ln\frac{1+\xi}{1-\xi}}{\sqrt{1-\xi^2}\,(x-\xi)}\,d\xi = x\int_{-1}^{1} \frac{\xi^{n-1} \ln\frac{1+\xi}{1-\xi}}{\sqrt{1-\xi^2}\,(x-\xi)}\,d\xi -$$

$$\pi\left[1-(-1)^{n-1}\right]\left(\frac{n}{2}-1\right)!\sum_{0}^{\frac{n}{2}-1}\frac{(-1)^{\nu}(1)(3)\ldots(\nu)}{2^{\nu}(2\nu+1)(\nu!)^2\left(\frac{n}{2}-1-\nu\right)!}$$

APPENDIX C

THE GERMAIN-WATSON-THWAITES-WEBER METHOD

The numerical procedure introduced by Germain (ref. 21) can be adapted to give approximately the thin-airfoil velocities on any profile in terms of its ordinates at certain fixed points. In the same way the airfoil slope and second derivative can be calculated. Thwaites has applied Germain's procedure to thin-airfoil theory (ref. 23), and Weber has systematized the calculation of the slope and surface velocity for uncambered airfoils (ref. 24). Here we must treat also cambered airfoils and find the second derivative. It is convenient to derive all these results from Watson's analysis (ref. 22).

Let $f(z)$ be regular within the unit circle, and on the unit circle have the form

$$f(e^{i\theta}) = R(\theta) + iI(\theta) \tag{C1}$$

(Our R and I are Watson's ψ and ϵ.) Then following Germain, Watson approximates to R by the trigonometric polynomial

$$R(\theta) \approx c_0 + \sum_{r=1}^{N-1} (c_r \cos r\theta + t_r \sin r\theta) + c_N \cos N\theta \tag{C2}$$

which can be made to coincide with R at the $2N$ equally spaced pivotal points $\theta = \theta_m = m\pi/N$. Thus he derives approximate formulas for I (aside from a constant), R', I', $\int R$, and $\int I$ in terms of the values of R at the pivotal points times fixed influence coefficients.

In thin-airfoil theory the complex perturbation potential $\varphi + i\psi$ is regular outside the unit circle in the absence of circulation. Inversion shows that this involves a change in sign of either the real or imaginary part, since $f(e^{-i\theta}) = R - iI$. Hence $(\varphi,-\psi)$ or (ψ,φ) may be identified with (R,I).

In thin-airfoil theory the tangency condition on the perturbation stream function ψ is $\psi = -Y$, where Y is the airfoil ordinate. Therefore, in order to obtain a solution in terms of the airfoil ordinates we identify $(Y,-\varphi)$ with (R,I).

Streamwise Velocity Increment

Let x run from 0 at the leading edge of the airfoil to 1 at the trailing edge, and

$$x = \frac{1}{2}(1 + \cos\theta) \tag{C3}$$

Then the streamwise perturbation velocity on the airfoil is given by

$$\frac{u}{U} = \frac{\partial\varphi}{\partial x} = \frac{\partial\varphi/\partial\theta}{dx/d\theta} = -\frac{2}{\sin\theta}\frac{\partial\varphi}{\partial\theta} \tag{C4}$$

Now according to Watson's equations (10), (24), and (27), in the absence of circulation the values of $\partial\varphi/\partial\theta$ at the points θ_m are

$$-\left(\frac{\partial\varphi}{\partial\theta}\right)_m = \sum_{p=0}^{2N-1}\beta_p Y_{m+p}, \qquad \beta_p = \begin{cases} \frac{1}{2}N, & p = 0 \\ 0, & p = \text{even, not } 0 \\ -\frac{1}{N(1-\cos\theta_p)}, & p = \text{odd} \end{cases} \tag{C5}$$

Now since $\beta_{2N-p} = \beta_p$,

$$\sum_{p=0}^{2N-1}\beta_p Y_{m+p} = \beta_m Y_0 + \sum_{p=1}^{N-1}\beta_{p-m}Y_p + \sum_{p=1}^{N-1}\beta_{p+m}Y_{2N-p} + \beta_{N-m}Y_N \tag{C6}$$

Symmetric airfoils.- For a symmetric airfoil $Y_{2N-p} = -Y_p$ and $Y_0 = Y_N = 0$. Then according to equations (C4), (C5), and (C6)

$$\frac{u_m}{U} = \sum_{p=1}^{N-1} c_{mp}Y_p, \qquad c_{mp} = \frac{2}{\sin\theta_m}(\beta_{p-m} - \beta_{p+m}) \tag{C7}$$

This form is convenient for calculating the c_{mp}. It is also easily shown, using trigonometric identities, that

$$c_{mp} = \begin{cases} \dfrac{N}{\sin \theta_m}, & p - m = 0 \\ 0, & p - m = \text{even, not } 0 \\ -\dfrac{4 \sin \theta_p}{N(\cos \theta_m - \cos \theta_p)^2}, & p - m = \text{odd} \end{cases} \tag{C8}$$

which is Weber's result.

Antisymmetric airfoils.- For a cambered airfoil of zero thickness $Y_{2N-p} = Y_p$. The ordinates Y_o and Y_N of the leading and trailing edges do not vanish in general, although in the present second-order theory the axis is chosen so that they do. Equation (C6) gives

$$\sum_{p=0}^{2N-1} \beta_p Y_{m+p} = \beta_m Y_o + \sum_{p=1}^{N-1} (\beta_{p-m} + \beta_{p+m}) Y_p + \beta_{N-m} Y_N \tag{C9}$$

This expression represents the velocity on the unit circle into which the airfoil is mapped. The Kutta condition will be violated at the trailing edge of the airfoil unless the expression happens to vanish for $m = 0$. Adding a component of circulatory flow changes the velocity on the circle by a constant. Hence the Kutta condition is enforced by subtracting from the expression of equation (C9) its value at $m = 0$, so that

$$\sum_{p=0}^{2N-1} \beta_p Y_{m+p} \rightarrow (\beta_m - \beta_o) Y_o + \sum_{p=1}^{N-1} (\beta_{p-m} + \beta_{p+m} - 2\beta_p) Y_p + (\beta_{N-m} - \beta_N) Y_N \tag{C10}$$

Hence, according to equations (C4) and (C5)

$$\frac{u_m}{U} = \sum_{p=0}^{N} d_{mp} Y_p, \qquad d_{mp} = \frac{2}{\sin \theta_m} \begin{cases} (\beta_m - \beta_o), & p = 0 \\ (\beta_{p-m} + \beta_{p+m} - 2\beta_p), & p \neq 0, N \\ (\beta_{N-m} - \beta_N), & p = N \end{cases} \tag{C11}$$

The expression for d_{mp} can be written more concisely in a form suitable for computation as

$$d_{mp} = \frac{2\nu}{\sin \theta_m} (\beta_{p-m} + \beta_{p+m} - 2\beta_p), \qquad \nu = \begin{cases} \frac{1}{2}, & p = 0, N \\ 1 \text{ otherwise} \end{cases} \tag{C12}$$

Slope of Airfoil

The airfoil slope is given by

$$Y' \equiv \frac{dY}{dx} = - \frac{2}{\sin \theta} \frac{dY}{d\theta} \tag{C13}$$

Now according to Watson's equations (29), (31), and (34)

$$\left(\frac{dY}{d\theta}\right)_m = \sum_{p=0}^{2N-1} \gamma_p Y_{m+p}, \qquad \gamma_p = \begin{cases} 0, & p = 0 \\ -\frac{1}{2} (-1)^p \frac{\sin \theta_p}{1 - \cos \theta_p}, & p \neq 0 \end{cases} \tag{C14}$$

or, since $\gamma_{2N-p} = - \gamma_p$

$$\left(\frac{dY}{d\theta}\right)_m = \sum_{p=0}^{N-1} \gamma_{p-m} Y_p - \sum_{p=1}^{N} \gamma_{p+m} Y_{2N-p} \tag{C15}$$

Symmetric airfoils.- Using the symmetry conditions again gives for symmetric airfoils

$$Y'_m = \sum_{p=1}^{N-1} e_{mp} Y_p, \qquad e_{mp} = - \frac{2}{\sin \theta_m} (\gamma_{p-m} + \gamma_{p+m}) \tag{C16}$$

Antisymmetric airfoils.- Similarly, for camber lines

$$Y'_m = \sum_{p=0}^{N} f_{mp} Y_p, \qquad f_{mp} = \frac{2\nu}{\sin \theta_m} (\gamma_{p+m} - \gamma_{p-m}) \tag{C17}$$

Second Derivative

The second derivative of the airfoil ordinate is given by

$$Y'' \equiv \frac{d^2Y}{dx^2} = \frac{4}{\sin^2\theta}\left(\frac{d^2Y}{d\theta^2} - \cot\theta\,\frac{dY}{d\theta}\right) \tag{C18}$$

An approximation for $d^2Y/d\theta^2$, which is required here, is found by extending Watson's analysis for the first derivative, as he suggests. Following closely his section 2.4 gives, after some computation,

$$\left(\frac{d^2Y}{d\theta^2}\right)_m = \sum_{p=0}^{2N-1} \mu_p Y_{m+p}, \qquad \mu_p = \begin{cases} -\dfrac{(N-1)(2N-1)}{6}, & p = 0 \\ (-1)^p\left(\dfrac{1}{2}N - \dfrac{1}{1-\cos\theta_p}\right), & p \neq 0 \end{cases} \tag{C19}$$

Symmetric airfoils.- By the foregoing procedure, it is found that for symmetric airfoils

$$Y''_m = \sum_{p=1}^{N} g_{mp} Y_p, \qquad g_{mp} = \frac{4}{\sin^2\theta_m}\left[(\mu_{p-m} - \mu_{p+m}) - \cot\theta_m(\gamma_{p-m} + \gamma_{p+m})\right] \tag{C20}$$

Antisymmetric airfoils.- Similarly, for camber lines

$$Y''_m = \sum_{p=0}^{N} h_{mp} Y_p, \qquad h_{mp} = \frac{4\nu}{\sin^2\theta_m}\left[(\mu_{p-m} + \mu_{p+m}) - \cot\theta_m(\gamma_{p-m} - \gamma_{p+m})\right] \tag{C21}$$

Tables

The six sets of influence coefficients required for calculating u/U, Y', and Y'' for both symmetric and antisymmetric airfoils are tabulated in tables II and III for $N = 8$. In addition, the coefficients required for calculating u/U are given in table V for $N = 16$. These values have been checked by applying them to a number of simple shapes - flat plate, ellipse, etc., - for which the approximation of the airfoil by

a trigonometric polynomial is exact. The values are believed to be accurate to within one unit in the last place.

For convenience of computation, the coefficients have been renumbered so that the pivotal points are counted from the leading to the trailing edge. This renumbering is indicated by using indices (n,s) rather than (m,p).

REFERENCES

1. Riegels, F., and Wittich, H.: Zur Berechnung der Druckverteilung von Profilen. Jan. 24, 1942. Aerodynamische Versuchsanstalt Göttingen E. V. Institut für theoretische Aerodynamik. Bericht 41/1/15.

2. Riegels, F.: Das Umströmungsproblem bei inkompressiblen Potentialströmungen. Ing.-Archiv., Bd. XVI, 1948, pp. 373-376, and Bd. XVII, 1949, pp. 94-106.

3. Keune, F.: Beiträge zur Profilforschung. VI. Zweite Näherung zur Berechnung der Geschwindigkeitsverteilung nach dem Singularitätenverfahren. Luftfahrtforschung, Bd. 20, Lfg. 6, June 1943, pp. 196-206.

4. Goldstein, Sydney: Low-drag and Suction Airfoils. Jour. Aero. Sci., vol. 15, no. 4, Apr. 1948, pp. 189-214.

5. Lighthill, M. J.: A New Approach to Thin Aerofoil Theory. Aero Quart., vol. 3, pt. 3, Nov. 1951, pp. 193-210.

6. Görtler, H.: Gasströmungen mit Übergang von Unterschall- zu Überschallgeschwindigkeiten. Z.a.M.M., Bd. 20, Heft 5, Oct. 1940, pp. 254-262.

7. Hantzsche, W., and Wendt, H.: Der Kompressibilitätseinfluss für dünne wenig gekrümmte Profile bei Unterschallgeschwindigkeit. Z.a.M.M., Bd. 22, Nr. 2, Apr. 1942, pp. 72-86.

8. Hantzsche, W.: Die Prandtl-Glauertsche Näherung als Grundlage für ein iterationsverfahren zur Berechnung kompressibler Unterschallströmungen. Z.a.M.M., Bd. 23, Heft 4, Aug. 1943, pp. 185-199.

9. Schmieden, C., and Kawalki, K. H.: Beitrage zum Umströmungsproblem bei hohen Geschwindigkeiten. Bericht S13, Teil 1, L.G.L., 1942, pp. 40-68. (Available in translation as NACA TM 1233, 1949.)

10. Kaplan, Carl: The Flow of a Compressible Fluid Past a Curved Surface. NACA Rep. 768, 1943.

11. Kaplan, Carl: The Flow of a Compressible Fluid Past a Circular Arc Profile. NACA Rep. 794, 1944.

12. Imai, Isao: Two-Dimensional Aerofoil Theory for Compressible Fluids. Rep. No. 294 (vol. 21, no. 9), Aero. Res. Inst., Tokyo Imperial Univ., May 1944, pp. 283-331. (Japanese text with English abstract)

13. Imai, Isao, and Oyama, Seiichi: The Third Approximation of the Thin-Wing Expansion Method for Compressible Fluids. Reps. Inst. of Sci. and Tech., Univ. Tokyo, vol. 2, nos. 3-4, Mar.-Apr. 1948, pp. 33-44. (Japanese text)

14. Van Dyke, Milton D.: A Study of Second-Order Supersonic Flow Theory. NACA Rep. 1081, 1952.

15. Keune, Friedrich: Das Tragflügel-Profil in der ebenen inkompressiblen und kompressiblen Strömung. Rapport FI 12, FI 13, Flygtekniska Institutionen, Kungl. Tekniska Högskolan, Stockholm, Feb.-May 1951.

16. Harder, Keith C., and Klunker, E. B.: On a Source-Sink Method for the Solution of the Prandtl-Busemann Iteration Equations in Two-Dimensional Compressible Flow. NACA TN 2253, 1950.

17. Hayes, Wallace D.: Second-Order Two-Dimensional Flow Theory and Imai's Similitude. British A.R.C. 15,722, F.M. 1877, 1953.

18. Imai, Isao: Extension of von Kármán's Transonic Similarity Rule. Jour. Phys. Soc. Japan, vol. 9, no. 1, Jan.-Feb. 1954, pp. 103-108.

19. Van Dyke, Milton D.: The Second-Order Compressibility Rule for Airfoils. Jour. Aero. Sci., vol. 21, no. 9, Sept. 1954, pp. 647-648.

20. Van Dyke, Milton D.: Subsonic Edges in Thin-Wing and Slender-Body Theory. NACA TN 3343, 1954.

21. Germain, P.: Sur le calcul numérique de certains opérateurs linéaires. Comptes Rendus Aca. Sci. Paris, vol. 220, 1945, pp. 765-768.

22. Watson, E. J.: Formulae for the Computation of the Functions Employed for Calculating the Velocity Distribution about a Given Aerofoil. R. & M. No. 2176, British A.R.C., 1945.

23. Thwaites, B.: A Method of Aerofoil Design. Part I - Symmetrical Aerofoils. R. & M. No. 2166, British A.R.C., 1945.

24. Weber, J.: The Calculation of the Pressure Distribution over the Surface of Two-Dimensional and Swept Wings with Symmetrical Aerofoil Sections. R.A.E. Rep. Aero. 2497, 1953.

25. Munk, Max M.: Elements of the Wing Section Theory and of the Wing Theory. NACA Rep. 191, 1924.

26. Goldstein, Sydney: Approximate Two-Dimensional Aerofoil Theory. Part I. Velocity Distributions for Symmetrical Aerofoils. C.P. 68, British A.R.C., 1942.

27. Jones, Robert T., and Cohen, Doris: Aerodynamics of Wings at High Speeds. Section A of vol. VII, Applied High-Speed Aerodynamics, High-Speed Aerodynamics and Jet Propulsion. Princeton Univ. Press. (In press)

28. Imai, Isao: Application of the M^2-Expansion Method to the Subsonic Flow of a Compressible Fluid Past a Parabolic Cylinder. Proc. 1st Japan Nat. Cong. Appl. Mech., 1952, pp. 349-352.

29. Kaplan, Carl: Two-Dimensional Subsonic Compressible Flow Past Elliptic Cylinders. NACA Rep. 624, 1938.

30. Allen, H. Julian: General Theory of Airfoil Sections Having Arbitrary Shape or Pressure Distribution. NACA Rep. 833, 1945.

31. Milne-Thomson, L. M.: Theoretical Hydrodynamics. Second ed., MacMillan Co., 1949.

32. Jacobs, Eastman N., Ward, Kenneth E., and Pinkerton, Robert M.: The Characteristics of 78 Related Airfoil Sections from Tests in the Variable-Density Wind Tunnel. NACA Rep. 460, 1933.

33. Goldstein, S.: Notes on "General Theory of Airfoil Sections Having Arbitrary Shape or Pressure Distribution," by H. Julian Allen. British A.R.C. Rep. No. 7142, F.M. 624, 1943.

34. Abbott, Ira H., von Doenhoff, Albert E., and Stivers, Louis S., Jr.: Summary of Airfoil Data. NACA Rep. 824, 1945.

35. Emmons, Howard W.: Flow of a Compressible Fluid Past a Symmetrical Airfoil in a Wind Tunnel and in Free Air. NACA TN 1746, 1948.

36. Graham, Donald J., Nitzberg, Gerald E., and Olsen, Robert N.: A Systematic Investigation of Pressure Distributions at High Speeds over Five Representative NACA Low-Drag and Conventional Airfoil Sections. NACA Rep. 832, 1945.

TABLE I.- PIVOTAL POINTS AND ANGLE-OF-ATTACK SOLUTION

N = 8			N = 16		
n	x_n	$\sqrt{\frac{1-x_n}{x_n}}$	n	x_n	$\sqrt{\frac{1-x_n}{x_n}}$
0	0	∞	0	0	∞
1	.038060	5.027339	1	.009607	10.15318
2	.146447	2.414214	2	.038060	5.027339
3	.308658	1.496606	3	.084265	3.296558
4	.500000	1.000000	4	.146447	2.414214
5	.691342	.668179	5	.222215	1.870868
6	.853553	.414214	6	.308658	1.496606
7	.961940	.198912	7	.402455	1.218504
8	1.000000	0	8	.500000	1.000000
			9	.597545	.820679
			10	.691342	.668179
			11	.777785	.532511
			12	.853553	.414214
			13	.915735	.303347
			14	.961940	.198912
			15	.990393	.098491
			16	1.000000	0

TABLE II.- INFLUENCE COEFFICIENTS FOR THICKNESS, N = 8.

c_{ns}

n \ s	1	2	3	4	5	6	7
1	20.90501	-4.07193	0	-0.22417	0	-0.07193	.0
2	-7.52395	11.31371	-3.35916	0	-.29769	0	-.13291
3	0	-4.38896	8.65914	-3.15432	0	-.38896	0
4	-.58579	0	-3.41421	8.00000	-3.41421	0	-.58578
5	0	-.38896	0	-3.15432	8.65914	-4.38896	0
6	-.13291	0	-.29769	0	-3.35916	11.31371	-7.52395
7	0	-.07193	0	-.22417	0	-4.07193	20.90501

e_{ns}

n \ s	1	2	3	4	5	6	7
1	-6.30865	-4.99321	1.53073	-0.82843	0.63405	-0.66364	1.08239
2	17.04789	-1.41421	-4.71832	2.00000	-1.40461	1.41421	-2.26582
3	-8.92177	8.05468	-.44834	-4.82842	2.61313	-2.39782	3.69552
4	5.65685	-4.00000	5.65685	0	-5.65685	4.00000	-5.65685
5	-3.69552	2.39782	-2.61313	4.82842	.44834	-8.05468	8.92177
6	2.26582	-1.41421	1.40461	-2.00000	4.71832	1.41421	-17.04789
7	-1.08239	.66364	-.63405	.82843	-1.53073	4.99321	6.30865

g_{ns}

n \ s	1	2	3	4	5	6	7
1	-414.3920	106.2602	-12.6863	3.5867	-1.3726	-0.2495	11.3137
2	99.4783	-160.0000	62.4057	-11.3137	3.8960	0	-23.0316
3	46.6274	76.5287	-97.6081	50.4692	-11.3137	2.0190	35.3137
4	-46.8824	-11.3137	54.0559	-84.0000	54.0559	-11.3137	-46.8824
5	35.3137	2.0190	-11.3137	50.4692	-97.6081	76.5287	46.6274
6	-23.0316	0	3.8960	-11.3137	62.4057	-160.0000	99.4783
7	11.3137	-.2495	-1.3726	3.5867	-12.6863	106.2602	-414.3920

TABLE III.- INFLUENCE COEFFICIENTS FOR CAMBER, N = 8

d_{ns}

s \ n	1	2	3	4	5	6	7
0	-8.58221	0	-0.43835	0	-0.19570	0	-0.33956
1	21.58414	-4.84984	.28130	-.32589	.28130	-.07193	.67913
2	-9.64046	11.31371	-3.75057	0	-.57900	0	-.81204
3	.94495	-4.38896	9.05055	-3.05260	.39141	-.24509	.94495
4	-1.53073	0	-3.69552	8.00000	-3.69552	0	-1.53073
5	2.11652	.38896	.87669	-2.60426	9.53583	-3.75490	2.11652
6	-.81204	0	-.57900	0	-3.75057	11.31371	-9.64046
7	17.16441	8.84984	7.10973	5.98275	7.10973	4.07193	38.06942
8	-21.24457	-11.31371	-8.85484	-8.00000	-9.09748	-11.31371	-29.48721

f_{ns}

s \ n	1	2	3	4	5	6	7
0	-13.13707	3.41421	-1.61991	1.00000	-0.72323	0.58579	-0.51978
1	6.30865	-9.22625	3.69552	-2.16478	1.53073	-1.22625	1.08239
2	9.22624	1.41421	-6.16478	2.82843	-1.83522	1.41421	-1.22625
3	-3.69552	6.16478	.44834	-5.22625	2.61313	-1.83522	1.53073
4	2.16478	-2.82843	5.22625	0	-5.22625	2.82843	-2.16478
5	-1.53073	1.83522	-2.61313	5.22625	-.44834	-6.16478	3.69552
6	1.22625	-1.41421	1.83522	-2.82843	6.16478	-1.41421	-9.22624
7	-1.08239	1.22625	-1.53073	2.16478	-3.69552	9.22625	-6.30865
8	.51978	-.58579	.72323	-1.00000	1.61991	-3.41421	13.13707

h_{ns}

s \ n	1		3	4	5	6	7
0	415.3214	-4.9706	-9.7012	12.0000	-16.0044	28.9706	-101.6159
1	-541.5880	80.1516	13.4903	-22.6274	31.4315	-57.5242	202.5097
2	68.1481	-120.0000	32.9909	16.0000	-29.1087	56.0000	-200.0304
3	144.5686	29.4458	-66.4121	22.6274	21.4903	-52.0732	194.5097
4	-181.8234	40.0000	21.8234	-56.0000	21.8234	40.0000	-181.8234
5	194.5097	-52.0732	21.4903	22.6274	-66.4121	29.4458	144.5686
6	-200.0304	56.0000	-29.1087	16.0000	32.9909	-120.0000	68.1481
7	202.5097	-57.5242	31.4315	-22.6274	13.4903	80.1516	-541.5880
8	-101.6159	28.9706	-16.0044	12.0000	-9.7012	-4.9706	415.3214

TABLE IV.- COMPRESSIBILITY FACTORS ($\gamma = 7/5$)

M	K_1	K_2	K_2-1	$\frac{K_2-1}{2}$
0	1.00000	1.00000	0	0
.10	1.00504	1.01016	.010162	.005081
.20	1.02062	1.04271	.042708	.021354
.25	1.03280	1.06933	.069333	.034667
.30	1.04828	1.10477	.104770	.052385
.35	1.06752	1.15129	.151294	.075647
.40	1.09109	1.21224	.212245	.106122
.45	1.11978	1.29260	.292603	.146302
.50	1.15470	1.40000	.400000	.200000
.55	1.19737	1.54654	.546545	.273272
.60	1.25000	1.75234	.752344	.376172
.65	1.31590	2.05275	1.05275	.526373
.70	1.40028	2.51465	1.51465	.757324
.75	1.51186	3.27755	2.27755	1.13878
.80	1.66667	4.67407	3.67407	1.83704
.85	1.89832	7.67085	6.67085	3.33543
.90	2.29416	16.1679	15.1679	7.58393
.95	3.20256	61.6651	60.6651	30.3325

NACA

TABLE V.- INFLUENCE COEFFICIENTS, N = 16.

c_{ns}

n / s	1	2	3	4	5	6	7	8	9	10	11	12	13	14	15
1	82.01330	-15.06135	0	-0.65117	0	-0.13634	0	-0.05070	0	-0.02624	0	-0.01712	0	-0.01344	0
2	-29.54391	41.81002	-11.20322	0	-.70527	0	-.18013	0	-.07641	0	-.04371	0	-.03105	0	-.02637
3	0	-16.26456	28.79924	-8.98045	0	-.68960	0	-.20090	0	-.09422	0	-.05867	0	-.04508	0
4	-2.36017	0	-11.42995	22.62742	-7.69823	0	-.67431	0	-.21718	0	-.11088	0	-.07468	0	-.06205
5	0	-1.53236	0	-9.05216	19.24304	-6.95446	0	-.67346	0	-.23613	0	-.13038	0	-.09497	0
6	-.64566	0	-1.14677	0	-7.72738	17.31827	-6.56330	0	-.69189	0	-.26237	0	-.15668	0	-.12424
7	0	-.46165	0	-.93529	0	-6.96756	16.31346	-6.44233	0	-.73451	0	-.30124	0	-.19583	0
8	-.25989	0	-.36162	0	-.80996	0	-6.56854	16.00000	-6.56854	0	-.80996	0	-.36162	0	-.25989
9	0	-.19583	0	-.30124	0	-.73451	0	-6.44233	16.31346	-6.96756	0	-.93529	0	-.46165	0
10	-.12424	0	-.15668	0	-.26237	0	-.69189	0	-6.56330	17.31827	-7.72738	0	-1.14677	0	-.64566
11	0	-.09497	0	-.13038	0	-.23613	0	-.67346	0	-6.95446	19.24304	-9.05216	0	-1.53236	0
12	-.06205	0	-.07468	0	-.11088	0	-.21718	0	-.67431	0	-7.69823	22.62742	-11.42995	0	-2.36017
13	0	-.04508	0	-.05867	0	-.09422	0	-.20090	0	-.68960	0	-8.98045	28.79924	-16.26456	0
14	-.02637	0	-.03105	0	-.04371	0	-.07641	0	-.18013	0	-.70527	0	-11.20322	41.81002	-29.54391
15	0	-.01344	0	-.01712	0	-.02624	0	-.05070	0	-.13634	0	-.65117	0	-15.06135	82.01330

d_{ns}

n / s	1	2	3	4	5	6	7	8	9	10	11	12	13	14	15
0	-66.69154	0	-2.67007	0	-0.67654	0	-0.31668	0	-0.21329	0	-0.19329	0	-0.24570	0	-0.64694
1	82.66025	-18.60789	.22718	-1.26820	.15179	-.33591	.12868	-.13368	.12865	-.06358	.15179	-.03167	.22718	-.01344	.64694
2	-37.14763	41.81002	-12.21573	0	-1.07882	0	-.39341	0	-.24027	0	-.20788	0	-.25823	0	-.67332
3	.69969	-17.37779	29.04494	-9.22666	.16417	-.76828	.13918	-.22511	.13918	-.09422	.16417	-.04412	.24570	-.01819	.69969
4	-5.24355	0	-11.98900	2.62742	-7.94982	0	-.83817	0	-.35636	0	-.26267	0	-.30185	0	-.76174
5	.82379	-1.92402	.28928	-9.12071	19.43633	-6.95446	.16386	-.64924	.16386	-.19878	.19329	-.08159	.28928	-.03170	.82379
6	-2.23771	0	-1.52330	0	-7.92067	17.31827	-6.70247	0	-.82058	0	-.41416	0	-.40238	0	-.94803
7	1.07227	-.46165	.37653	-.86673	.25159	-6.88888	16.52674	-6.35935	.21329	-.64470	.25159	-.19844	.37653	-.06915	1.07227
8	-1.33216	0	-.65089	0	-.97413	0	-6.65723	16.00000	-6.69723	0	-.97413	0	-.65089	0	-1.33216
9	1.59205	.19583	.55905	-.05504	.37355	-.53494	.31668	-6.25795	16.63014	-6.77912	.37355	-.72333	.55905	-.19666	1.59205
10	-.94803	0	-.40238	0	-.41416	0	-.82058	0	-6.70247	17.31827	-7.92067	0	-1.52330	0	-2.23771
11	2.88338	1.01826	1.01251	.48665	.67654	.23613	.57354	-.24744	.57354	-6.51954	19.91958	-8.55247	1.01251	-.87405	2.88338
12	-.76174	0	-.30185	0	-.26267	0	-.35636	0	-.83817	0	-7.94982	22.62742	-11.98900	0	-5.24355
13	7.60372	3.50146	2.67007	1.86070	1.78408	1.36367	1.51247	1.12180	1.51247	.68960	1.78408	-7.32184	31.46931	-13.85815	7.60372
14	-.67332	0	-.25823	0	-.20788	0	-.24027	0	-.34341	0	-1.07882	0	-12.21473	41.81002	-37.14763
15	66.69154	33.65379	23.41895	18.18999	15.64805	13.88267	13.26577	12.75098	13.26577	13.61034	15.64805	16.95346	23.41895	15.06135	148.70484
16	-164.67355	-83.62003	-57.84418	-45.25483	-38.67937	-34.63654	-32.84020	-32.00000	-32.94359	-34.63654	-39.16262	-45.25483	-60.26855	-83.62003	-230.71815

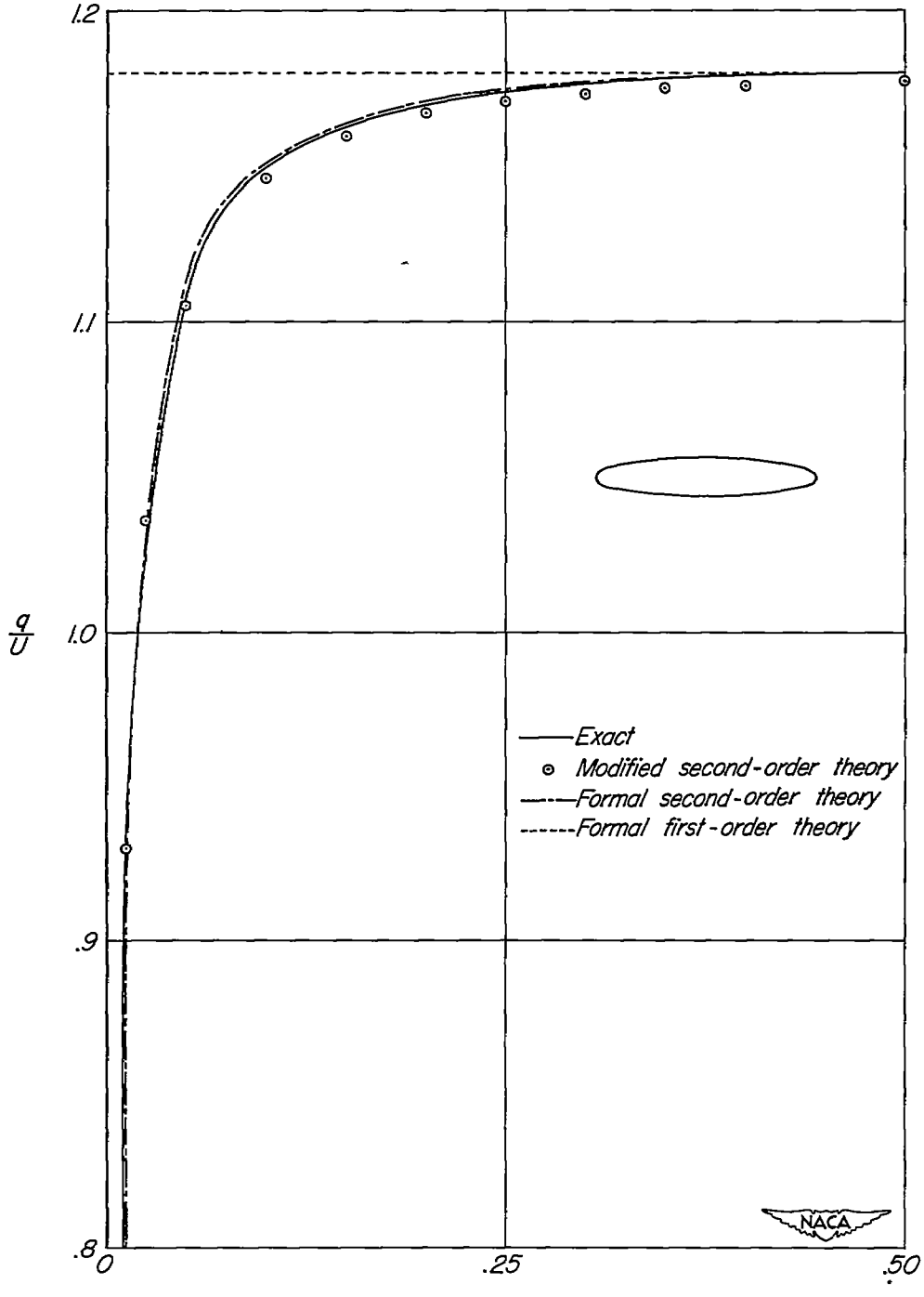

Figure 1. - Speed on 18-percent-thick ellipse at zero angle of attack in incompressible flow.

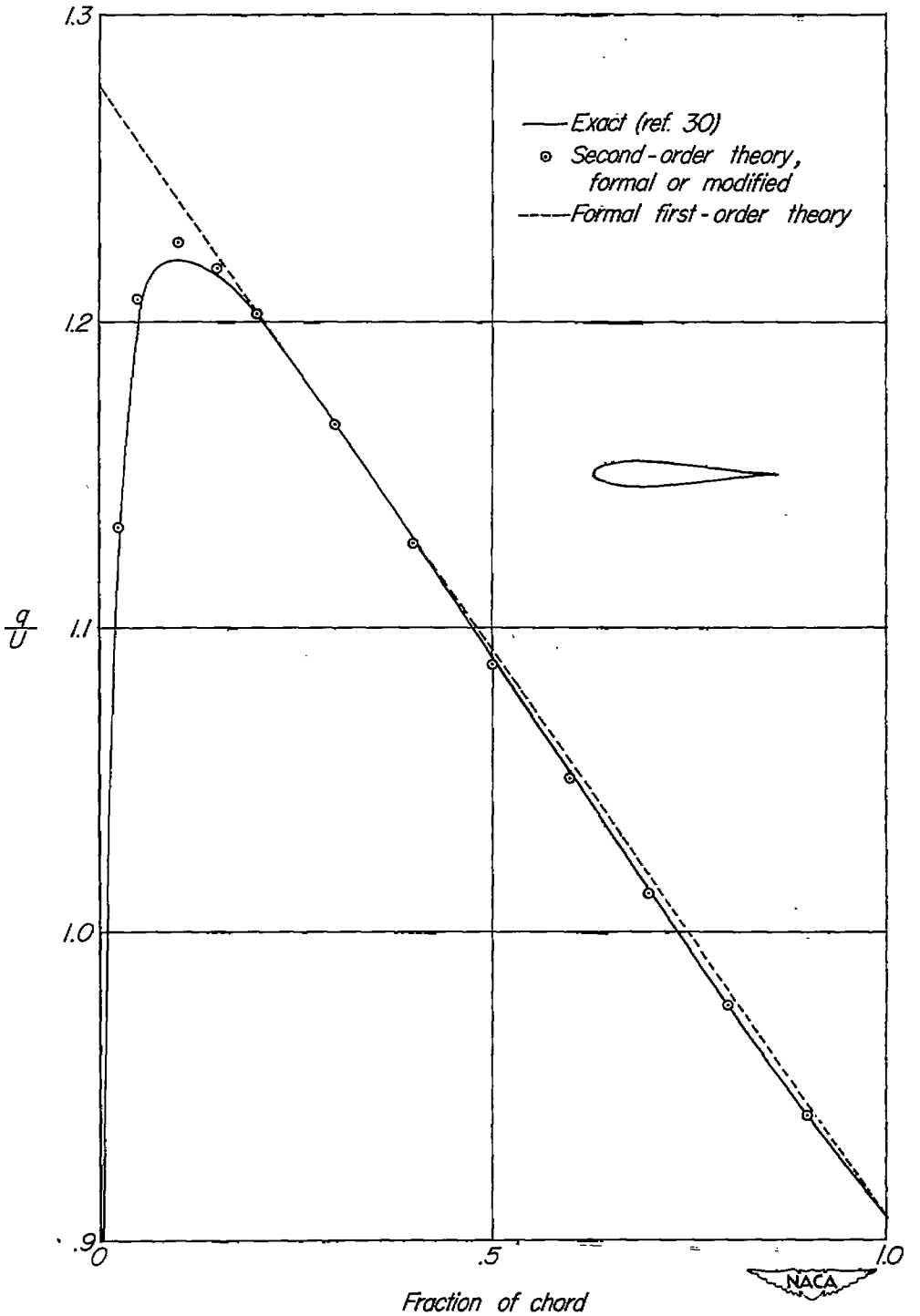

Figure 2.- Speed on 12-percent-thick symmetrical Joukowski airfoil at zero angle of attack in incompressible flow.

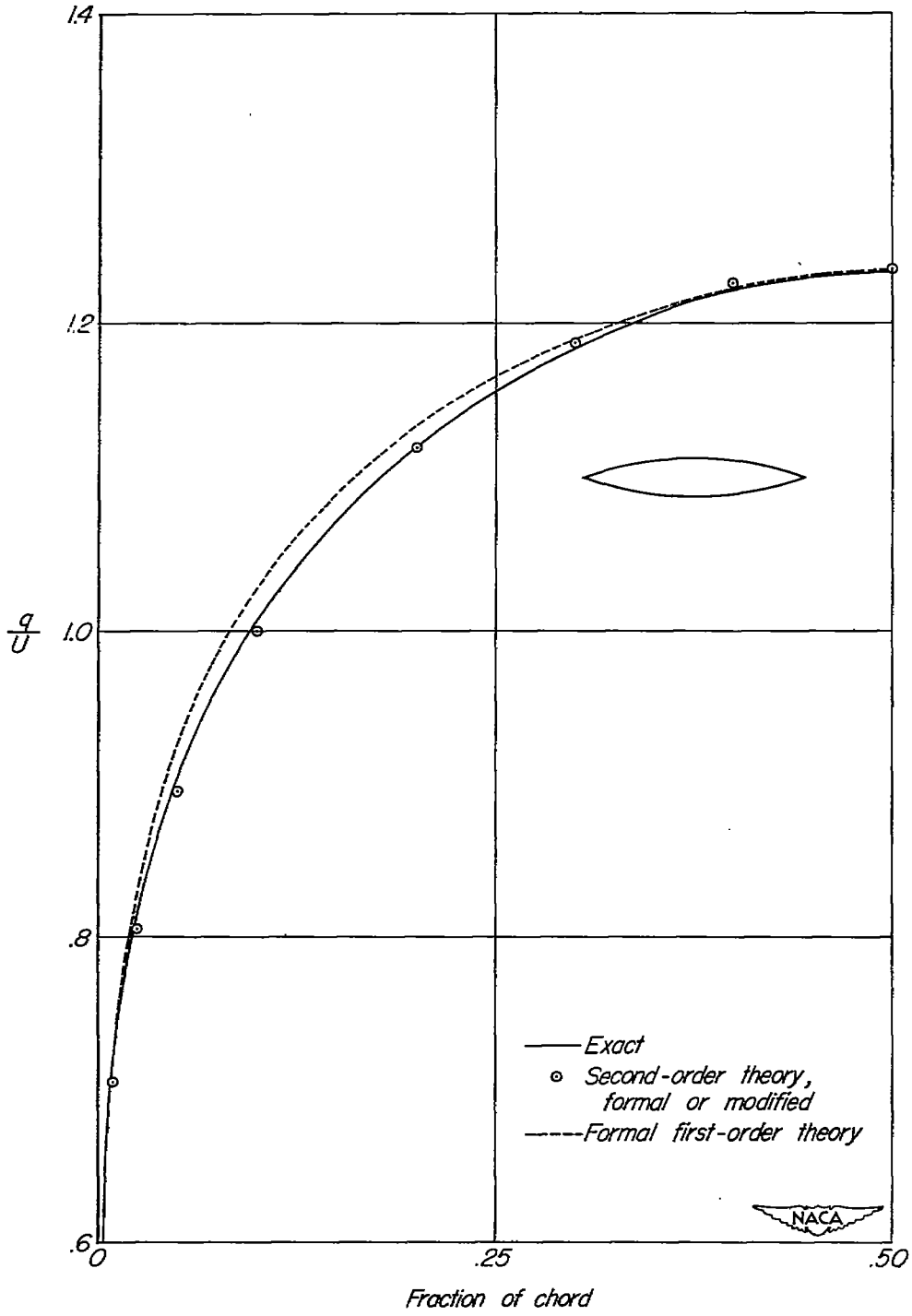

Figure 3.- Speed on 18-percent-thick biconvex airfoil at zero angle of attack in incompressible flow.

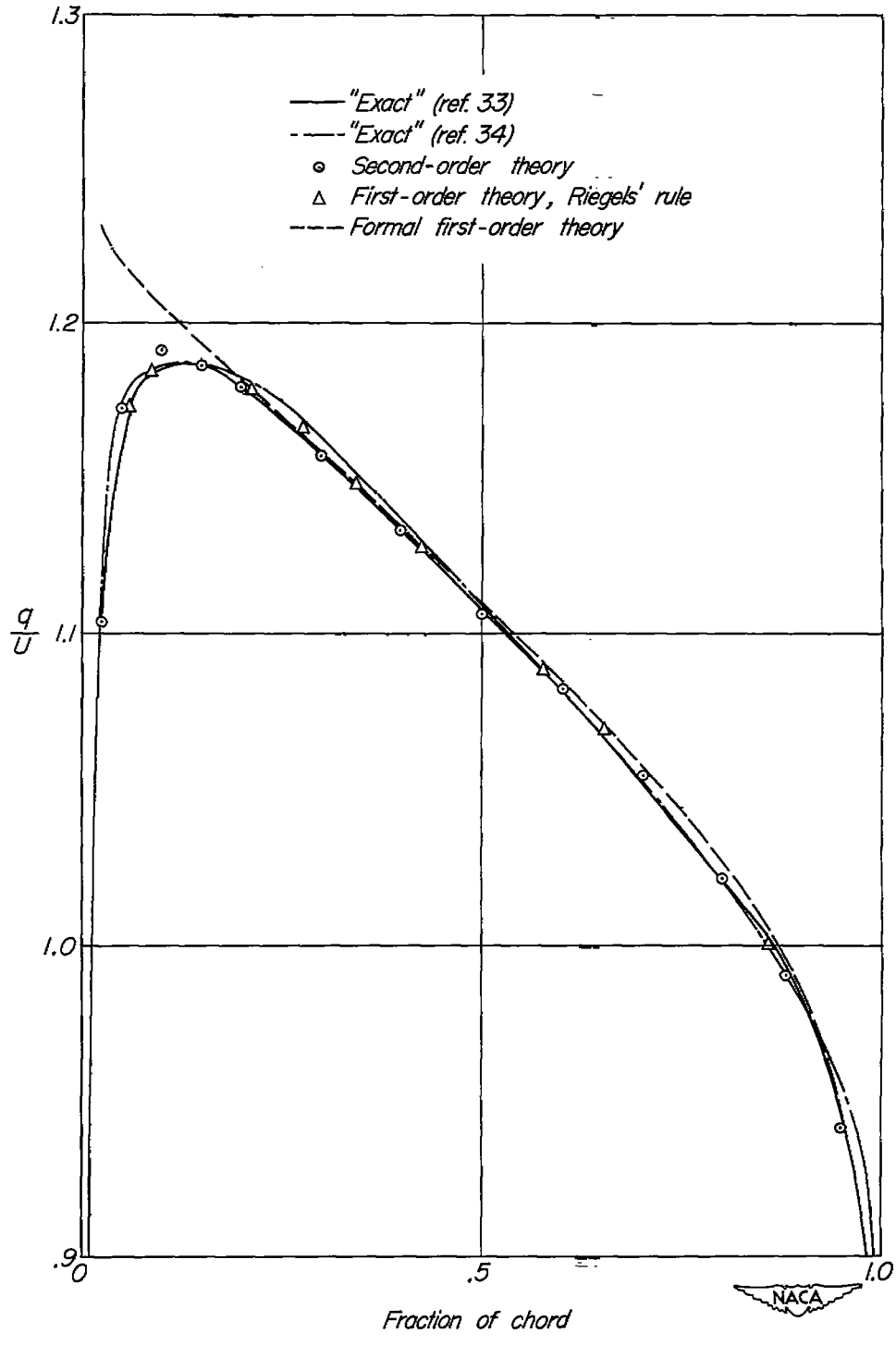

Figure 4.- Speed on NACA 0012 airfoil at zero angle of attack in incompressible flow.

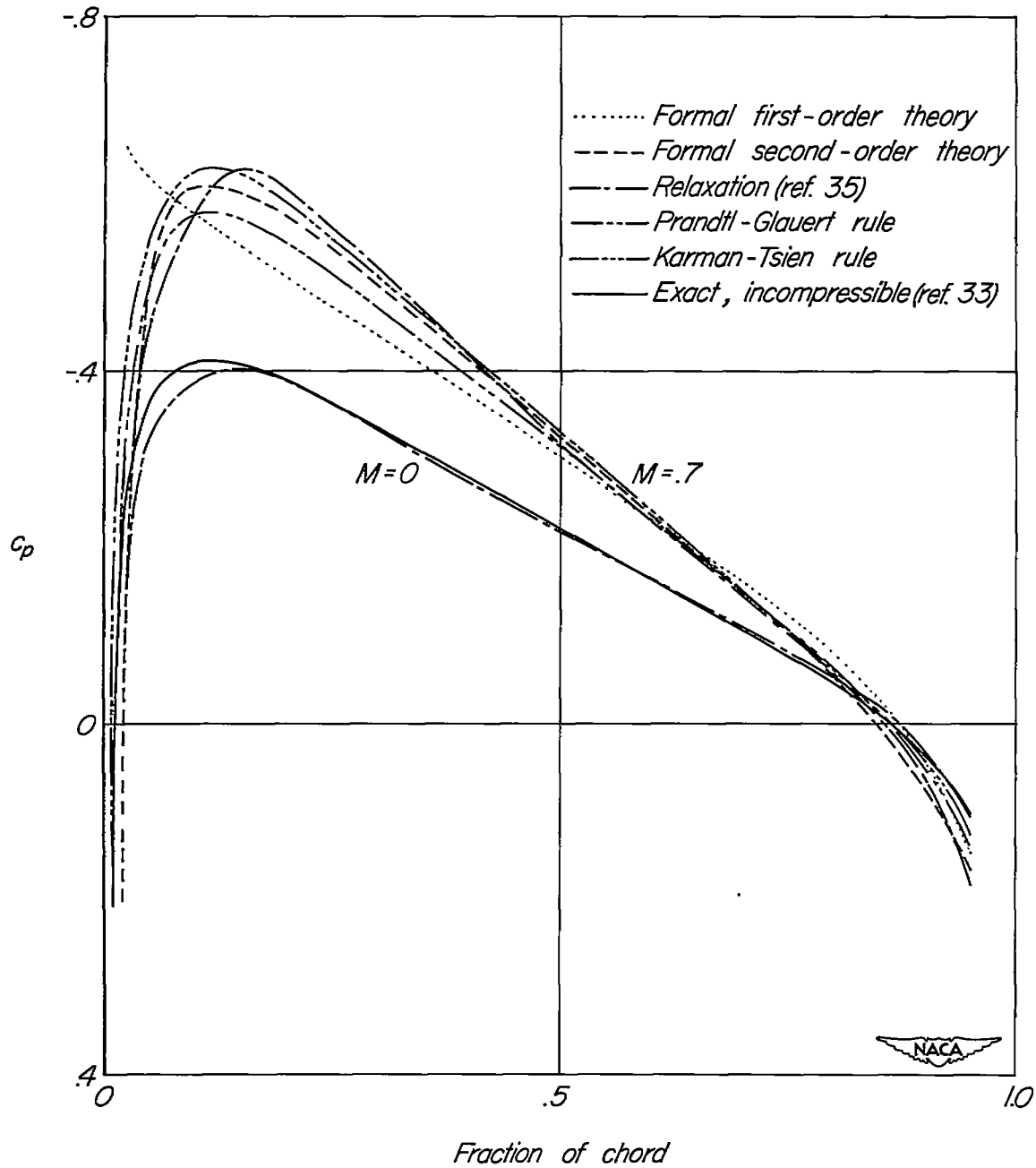

Figure 5.- Pressure coefficient on NACA 0012 airfoil at zero angle of attack in subsonic flow.

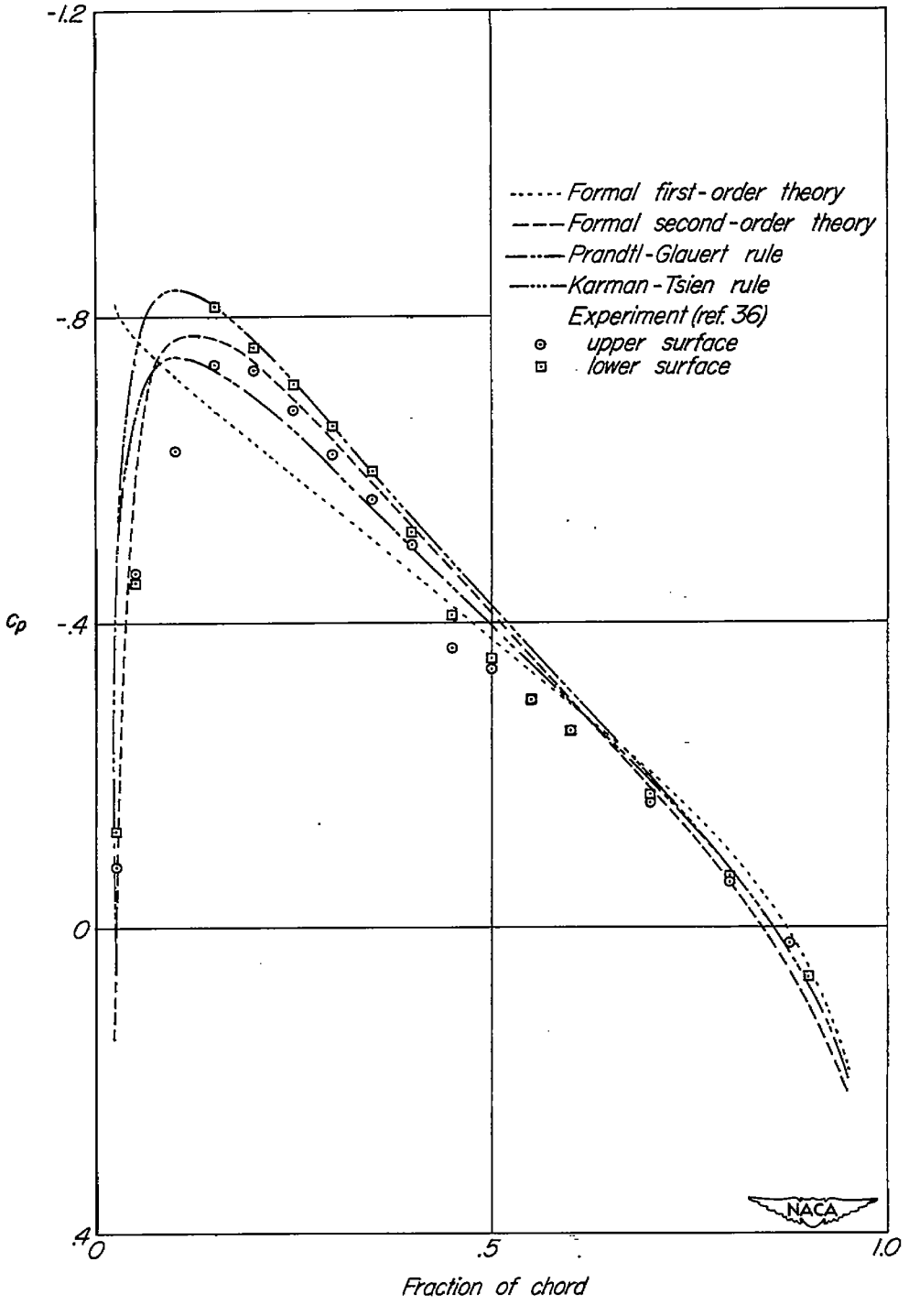

Figure 6.- Comparison of theoretical and experimental pressure distributions on NACA 0015 airfoil at M=0.70, zero angle of attack.

NACA-Langley - 3-14-55 - 1000